

NACA RM L56I25



# RESEARCH MEMORANDUM

AERODYNAMIC FORCES AND MOMENTS ON A LARGE OGIVE-CYLINDER

STORE AT VARIOUS LOCATIONS BELOW THE FUSELAGE CENTER

LINE OF A SWEEP-WING BOMBER CONFIGURATION

AT A MACH NUMBER OF 1.61

By Odell A. Morris

Langley Aeronautical Laboratory  
Langley Field, Va.

**DECLASSIFIED - EFFECTIVE 1-15-68**  
Authority: Memo Geo. Drobnik NASA HQ.  
Date 8/28-8 Dtd. 3-12-61; Subj: Change  
in Security Classification Marking.

GPO PRICE \$	_____
OTS PRICE(S) \$	_____
Hard copy (HC)	2.00
Microfiche (MF)	50

## NATIONAL ADVISORY COMMITTEE FOR AERONAUTICS

WASHINGTON

January 14, 1957

X-1325

N65-12717  
(ACCESSION NUMBER)  
45  
(PAGES)

(NASA CR OR TMX OR AD NUMBER)

(THRU)  
(CODE)  
01  
(CATEGORY)

FACILITY

DECLASSIFIED

NATIONAL ADVISORY COMMITTEE FOR AERONAUTICS

RESEARCH MEMORANDUM

AERODYNAMIC FORCES AND MOMENTS ON A LARGE OGIVE-CYLINDER

STORE AT VARIOUS LOCATIONS BELOW THE FUSELAGE CENTER

LINE OF A SWEEP-WING BOMBER CONFIGURATION

AT A MACH NUMBER OF 1.61

By Odell A. Morris

DECLASSIFIED - EFFECTIVE 1-15-64  
Authority: Memo Geo. Drobka NASA HQ,  
Code ATSS-A Dtd. 3-11-64 Subj: Changes  
in Security Classification Markings

SUMMARY

12717  
A supersonic wind-tunnel investigation on store interference has been conducted in the Langley 4- by 4-foot supersonic pressure tunnel at a Mach number of 1.61. Forces and moments were measured on a large ogive-cylinder store in the presence of a 45° swept-wing-fuselage bomber configuration for a number of store locations below the fuselage center line.

Results of the investigation show that large variations of store lift, drag, and pitch occur with changes in store or airplane angle of attack, store vertical location, and store horizontal location. The variation of the store forces and moments with respect to the chordwise location of the wing plan form indicates that the wing is a large factor in producing the interference loads on the store. Comparison of data for underfuselage and underwing store locations at an angle of attack of 0° showed maximum store drag interferences of similar magnitudes, but showed considerably smaller maximum interference on store lift and pitching moments for underfuselage store locations.

*Author*

INTRODUCTION

At transonic and supersonic speeds, research on external stores and nacelles has shown that interference from the various aircraft components may lead to large performance penalties. In recognition of the need for additional data on stores, a detailed investigation of store interference at supersonic speeds has been made in the Langley 4- by 4-foot supersonic pressure tunnel. (See refs. 1 to 3.)

[Redacted]

References 1 and 2 present results of tests made on a  $45^\circ$  swept-wing bomber configuration with a large ogive-cylinder store for a large number of underwing store locations. The present investigation supplements the data of references 1 and 2 with additional tests made for a number of store horizontal and vertical locations below the fuselage center line of a geometrically similar  $45^\circ$  swept-wing—fuselage combination. The aerodynamic characteristics of the store, without pylon, were measured for a range of angle of attack between  $\pm 8^\circ$  at a Mach number of 1.61. The results of these tests are presented herein and are compared with the underwing store data of references 1 and 2. Sufficient data were obtained to permit presentation in contour map form. From the contour plots, calculation of the store-release characteristic, as outlined in reference 4, may be made for the underfuselage conditions.

## SYMBOLS

$C_{D_s}$	drag coefficient of store (uncorrected for base drag), $\frac{\text{Drag}}{qF}$
$C_{L_s}$	lift coefficient of store, $\frac{\text{Lift}}{qF}$
$C_{m_s}$	pitching-moment coefficient of store, about store nose, $\frac{\text{Pitching moment}}{qFl}$
$l$	length of store, 13.1 in.
$q$	dynamic pressure, $\frac{1b}{\text{sq ft}}$
$F$	maximum frontal area of store, 0.0147 sq ft
$d$	store diameter, 1.64 in.
$x$	horizontal (streamwise) distance between store midpoint and fuselage nose (See fig. 1.)
$x_w$	chordwise location of store midpoint, measured from leading edge of wing center-line chord, in.
$c$	wing center-line chord, 10.07 in.
$\bar{c}$	mean aerodynamic chord, 7.18 in.
$b$	wing span, 26.18 in.



- y spanwise location of store center line, measured from fuselage center line, in.
- z vertical distance between store midpoint and fuselage center line at 22-inch station, in.
- h' vertical distance between store midpoint and fuselage surface, in.
- $\alpha_s$  angle of attack of store measured with respect to free airstream, deg
- $\alpha_{wf}$  angle of attack of wing-fuselage combination measured with respect to free airstream, deg

#### APPARATUS AND TESTS

The principal dimensions of the models and the general arrangement of the test setup are shown in figure 1. The  $45^\circ$  swept-wing-fuselage-store combination was designed to simulate a heavy-bomber airplane with a large external store. This configuration was geometrically similar to that used in references 1 and 2.

The wing and fuselage were constructed of steel and were sting mounted in the Langley 4- by 4-foot supersonic pressure tunnel with the wings in a vertical plane. This support system allowed the model to be traversed in the X and Z axes and pitched through an angle-of-attack range. The ogive-cylinder store was constructed of aluminum and was mounted on a six-component strain-gage balance with a separate support strut which was cantilevered from the tunnel side wall as shown in figure 1. For each of the store positions shown on the grid of figure 1, tests were made with store angles of  $0^\circ$ ,  $\pm 4^\circ$ , and  $\pm 8^\circ$ , except where it was physically impossible. Tests were made for four different chordwise locations by manually adjusting the length of the wing-fuselage sting during shutdown between runs. Reference 4 describes in detail the test technique and gives a discussion of the problems encountered. The variation of the store attitude due to aerodynamic deflection under load is small (about the same order of magnitude as the variations shown in ref. 1) and no corrections have been applied to the nominal store angles. In order to insure a turbulent boundary layer for all tests, a 1/4-inch-wide strip of no. 60 carborundum grains and shellac was located on both surfaces of the wing at the 10-percent-chord line and on the fuselage and store nose 1/2 inch from the tip.





## ACCURACY OF DATA

An estimate of the relative accuracy in the present data which was determined from an inspection of repeat test points and static-calibration deflections is as follows:

## Wing-fuselage:

$\alpha_{wf}$ , deg . . . . .  $\pm 0.10$

## Store:

x, in. . . . .  $\pm 0.05$

z, in. . . . .  $\pm 0.10$

$\alpha_s$ , deg . . . . .  $\pm 0.10$

$C_{L_s}$  . . . . .  $\pm 0.02$

$C_{D_s}$  . . . . .  $\pm 0.01$

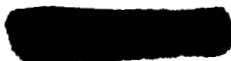
$C_{m_s}$  . . . . .  $\pm 0.02$

## RESULTS AND DISCUSSION

The lift, drag, and pitching-moment coefficients for the isolated store are presented in figure 2 for angles of attack up to  $8\frac{1}{2}^\circ$ . These results are in excellent agreement with the isolated-store data of reference 1, which were obtained using a different model and balance. The basic data for the store tested in the presence of the  $45^\circ$  swept-wing-fuselage combination are shown in figures 3 to 5. Store drag (fig. 3), lift (fig. 4), and pitching-moment coefficients (fig. 5) are presented plotted against the store vertical location  $z$  for several horizontal locations  $x$  and for various combinations of angle of attack of the wing-fuselage configuration and store. The pitching moments were computed about the nose of the store and all drag data are uncorrected for base pressure.

The data of figure 6 show the effects of store horizontal location on store lift, drag, and pitching-moment coefficients for three store vertical locations. These figures were obtained from cross plots of the basic data for equal angles of attack on the wing-fuselage-store combination and at equal store vertical heights (referenced to the fuselage center line) for each horizontal location.

Although this store is somewhat large for locations under the fuselage, the data for small vertical heights give an indication of the magnitudes and trends of the interferences encountered for fuselage-mounted stores. The effects of a support pylon on the aerodynamic characteristics of the store have not been determined; however, with proper design



it seems improbable that its interference would significantly alter these results. The data of figure 6 show that large variation of store lift, drag, and pitching-moment coefficients occurs with changes in store horizontal location, store angle of attack, and store vertical height, particularly for  $4^\circ$  and  $8^\circ$  angle of attack. For all coefficients, the variation of the interference is of considerably less magnitude at  $\alpha = 0^\circ$ , and the curves for the  $0^\circ$  case are quite different in character from the curves at  $4^\circ$  and  $8^\circ$  angle of attack. (See fig. 6(a).) An examination of the flow field in a manner similar to the pressure field analysis of reference 1 indicates that the low lift and drag and the high pitching moments shown at  $4^\circ$  and  $8^\circ$  angles of attack for forward store position are a result of the presence of the store afterbody in a strong positive pressure region originating from the wing. Conversely, the high forces and negative moments for the rearward store locations are a result of the same region of flow acting on the store nose. At an angle of attack of  $0^\circ$ , the intensity of the wing pressure field is considerably less; consequently, interference of the fuselage pressure field on the wing pressure field more nearly compensates each other resulting in curves of a different nature with smaller chordwise variations.

When the store vertical height  $h'$  was increased from 1.12 to 3.08, the magnitudes of store lift, drag, and pitching-moment coefficients changed but, in general, showed chordwise variations of a similar nature (figs. 6(b) and 6(c)).

#### Spanwise Contour Plots

Figures 7 to 9 present spanwise contour plots of store drag, lift, and pitching-moment coefficients which utilize store data from the present tests for the full-span bomber configuration and from references 1 and 2 for the semispan bomber configuration. For these plots, the point at which the value of store coefficient is plotted is the store midpoint and the intersection of the grid lines represents actual store test points. The store vertical heights compared for the two different tests are referenced from the store midpoint to the wing or fuselage surface. (See sketch in each figure.) Although the contour fairing between the underwing store locations ( $\frac{y}{b/2} = 0.25$ ) and the fuselage-center-line store locations ( $\frac{y}{b/2} = 0$ ) is strictly arbitrary, the figures are interesting insofar as showing trends and for comparing the magnitudes of the coefficients for the two different tests.

The drag data of figure 7(a) show that maximum store drag occurs for inboard underwing store positions. Figure 7(b) showed that increasing the store vertical height to  $\frac{h'}{d} = 1.24$  caused the maximum drag of



the store to occur for store locations along the fuselage center line near the wing trailing edge; however, the maximum drag coefficients were essentially independent of spanwise locations. The drag for fuselage store locations forward and rearward of the wing plan form tends to decrease toward or below the isolated store drag in the same fashion as shown for underwing locations. The contour plots of figures 8 and 9 show that the maximum store lift and pitching-moment coefficients for stores located below the fuselage center line at both vertical heights are considerably smaller than the maximum coefficients obtained for underwing store locations. Also as was noted for store drag coefficients, the lift and pitching-moment coefficients tend to decrease toward or below the isolated store values for store locations below the fuselage center line forward and rearward of the wing plan form. Hence, the underfuselage contour data show trends similar to those previously shown for underwing store locations, and thus indicate that the wing is a large factor in the productions of the interferences on the store for store locations below the fuselage center line. However, the maximum interference values of lift and pitch for the underfuselage store locations are smaller and farther rearward, evidently due to the fact that the store is actually a considerably greater distance from the wing.

#### Vertical Contour Plots

Vertical contour plots for store drag, lift, and pitching moments are presented in figures 10 to 12 for the wing-fuselage angle of attack of  $4^\circ$  with various store angles of attack up to  $\pm 8^\circ$ . Similar plots for any of the angles tested can be made from the basic data (figs. 3 to 5). For these figures also, the point at which the value of the store coefficient is plotted is the store midpoint. As shown in the figures,  $z$  is the vertical distance between the fuselage center line at station 22 and the store midpoint.

In general, the contour plots show rapid variations of the store forces and moments with  $x$  and  $z$ . Data in this form may be used directly in determining the store-release characteristics by calculating the drop path as outlined in reference 4. By using this method, the trajectory of the store following release may be calculated by a step-wise process.

#### CONCLUDING REMARKS

Forces and moments have been measured at a Mach number of 1.61 on a store in the presence of a  $45^\circ$  swept-wing-fuselage bomber configuration for a number of store locations below the fuselage center line. Results of the investigations show that large variations of store lift,



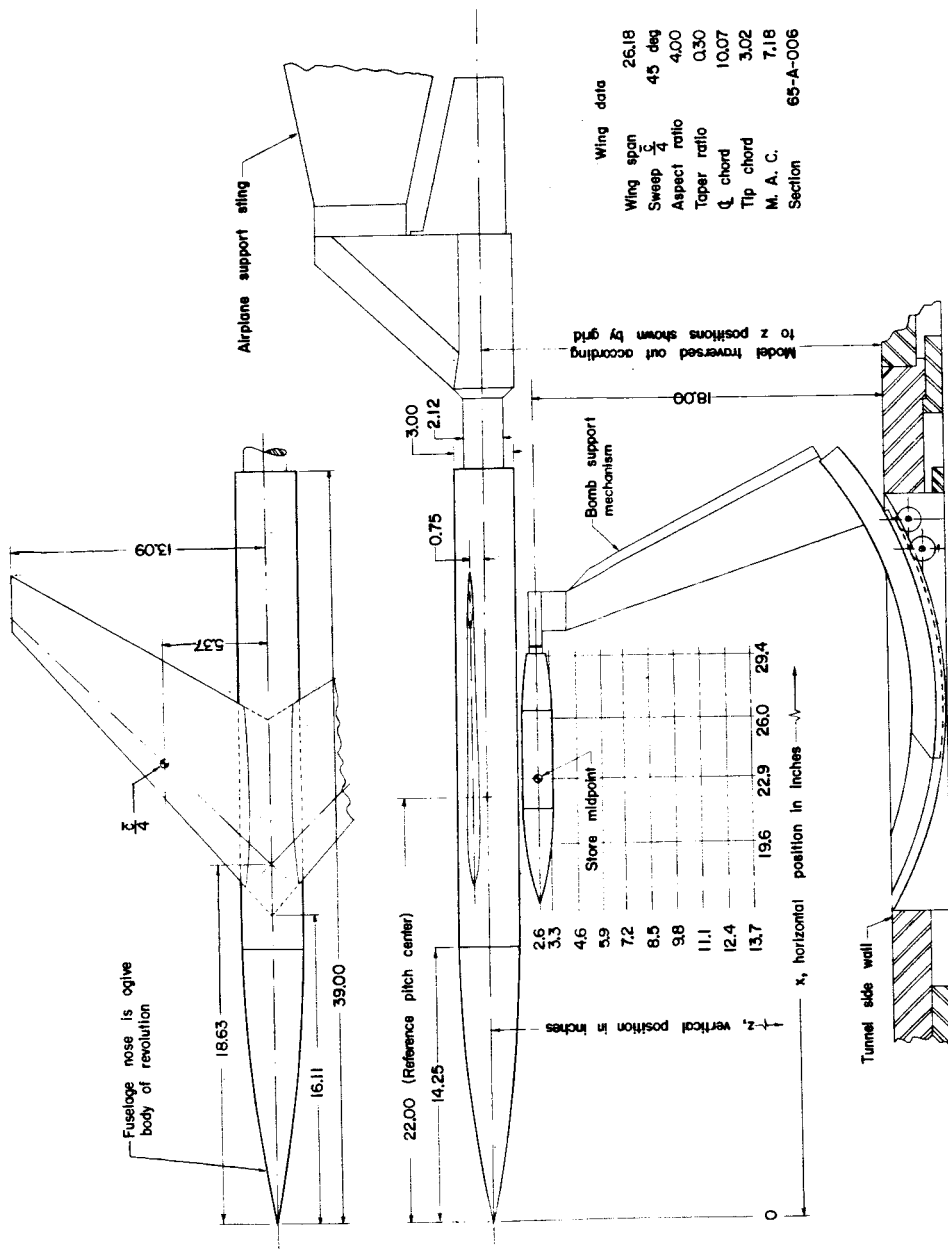
drag, and pitching-moment coefficients occur with changes in store or airplane angle of attack and with changes in store vertical and horizontal locations. The variation of the store forces and moments with respect to the chordwise location of the wing plan form indicates that the wing is a large factor in producing the interference loads on the store. Comparison of data for underfuselage and underwing store locations at an angle of attack of  $0^\circ$  showed maximum drag interferences of similar magnitudes, but showed considerably smaller maximum interference on store lift and pitching moments for underfuselage store locations.

Langley Aeronautical Laboratory,  
National Advisory Committee for Aeronautics,  
Langley Field, Va., September 4, 1956.

[REDACTED]

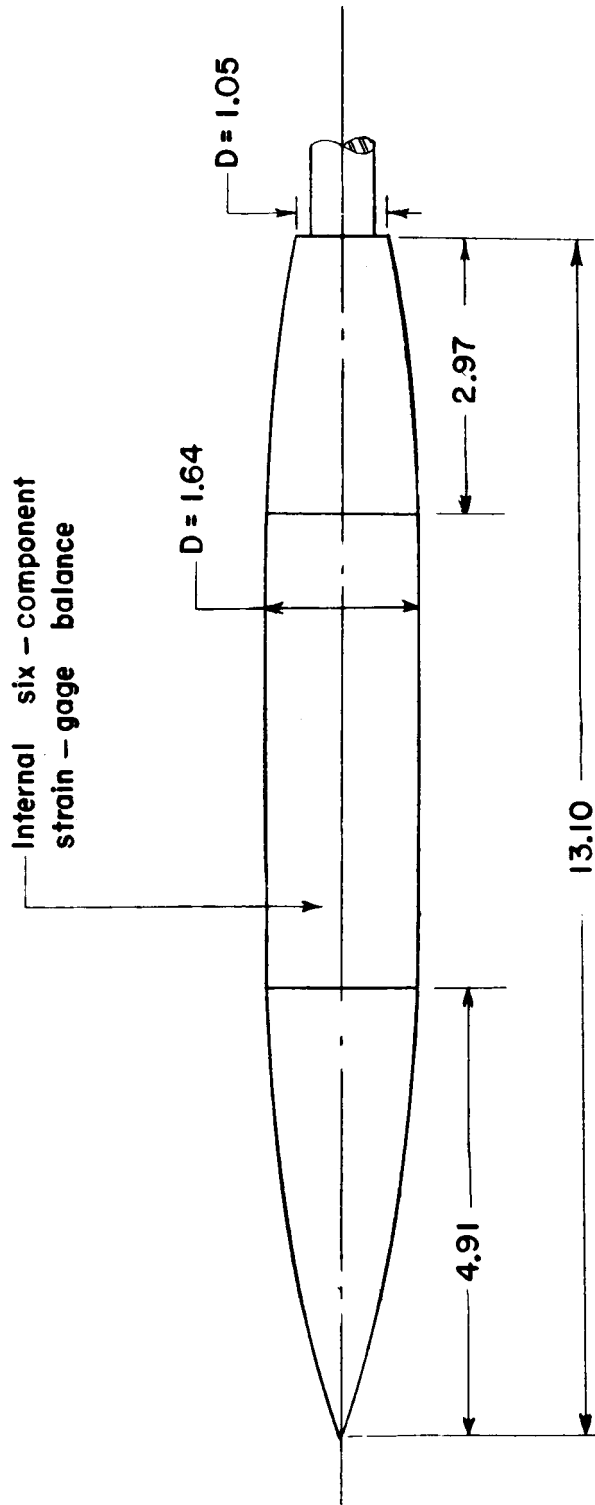
## REFERENCES

1. Smith, Norman F., and Carlson, Harry W.: The Origin and Distribution of Supersonic Store Interference From Measurement of Individual Forces on Several Wing-Fuselage-Store Configurations. I.- Swept-Wing Heavy-Bomber Configuration With Large Store (Nacelle). Lift and Drag; Mach Number 1.61. NACA RM L55A13a, 1955.
  2. Smith, Norman F., and Carlson, Harry W.: The Origin and Distribution of Supersonic Store Interference From Measurement of Individual Forces on Several Wing-Fuselage-Store Configurations. II.- Swept-Wing Heavy-Bomber Configuration With Large Store (Nacelle). Lateral Forces and Pitching Moments; Mach Number 1.61. NACA RM L55E26a, 1955.
  3. Smith, Norman F.: The Origin and Distribution of Supersonic Store Interference From Measurement of Individual Forces on Several Wing-Fuselage-Store Configurations. VI.- Swept-Wing Heavy-Bomber Configuration With Stores of Different Sizes and Shapes. NACA RM L55L08, 1956.
  4. Smith, Norman F., and Carlson, Harry W.: Measurement of Static Forces on Internally Carried Bombs of Three Fineness Ratios in Flow Field of a Swept-Wing Fighter-Bomber Configuration at a Mach Number of 1.61 With Illustrative Drop-Path Calculations. NACA RM L56I18, 1956.
- 



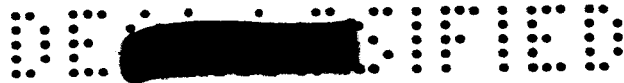
(a) Layout of wing-fuselage combination showing dimensions of components and store locations investigated.

Figure 1.- Details of models and supports. (All dimensions in inches.)



(b) Dimensions of store. Store nose and afterbody are ogive bodies of revolution. Center section is cylindrical.

Figure 1.- Concluded.



- Isolated store data (present tests)
- Isolated store data (refs. 1 and 2)

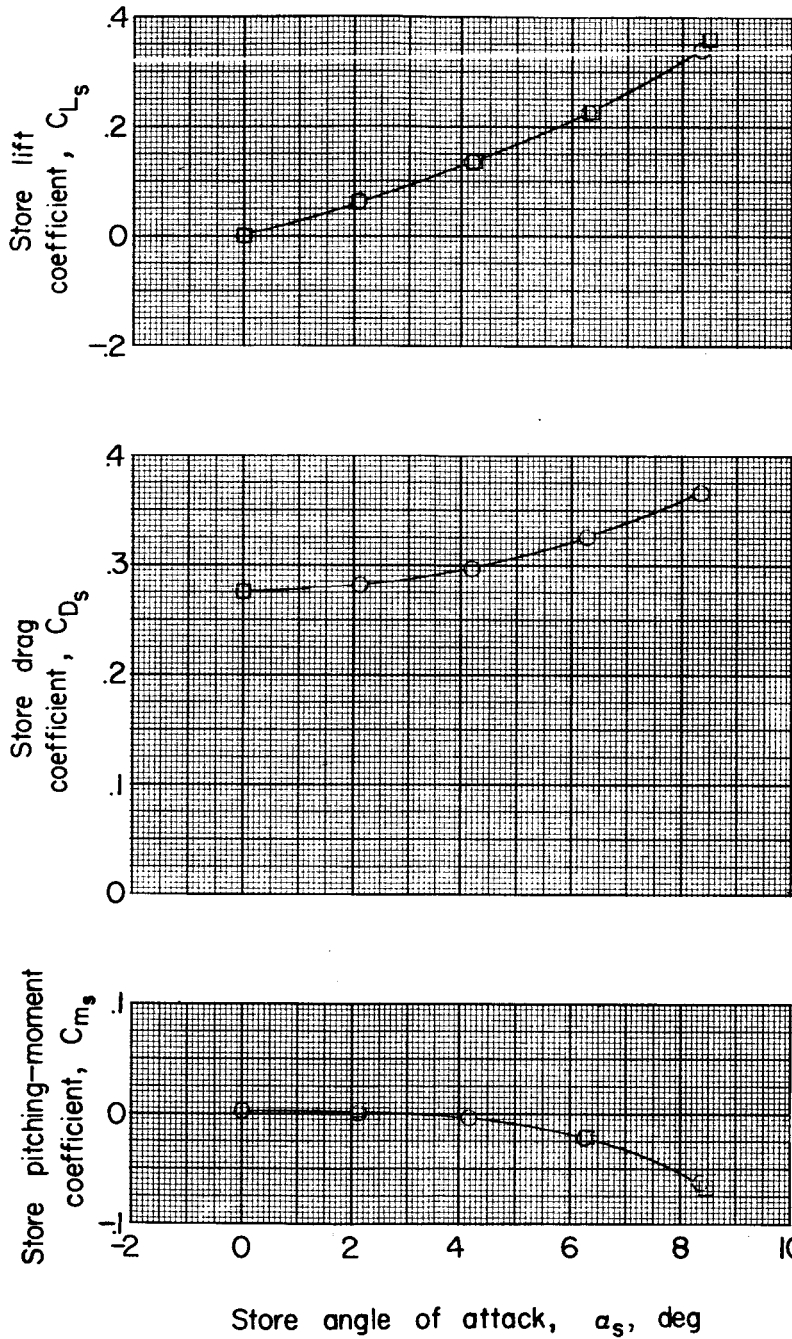
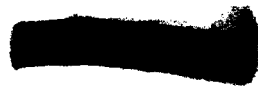
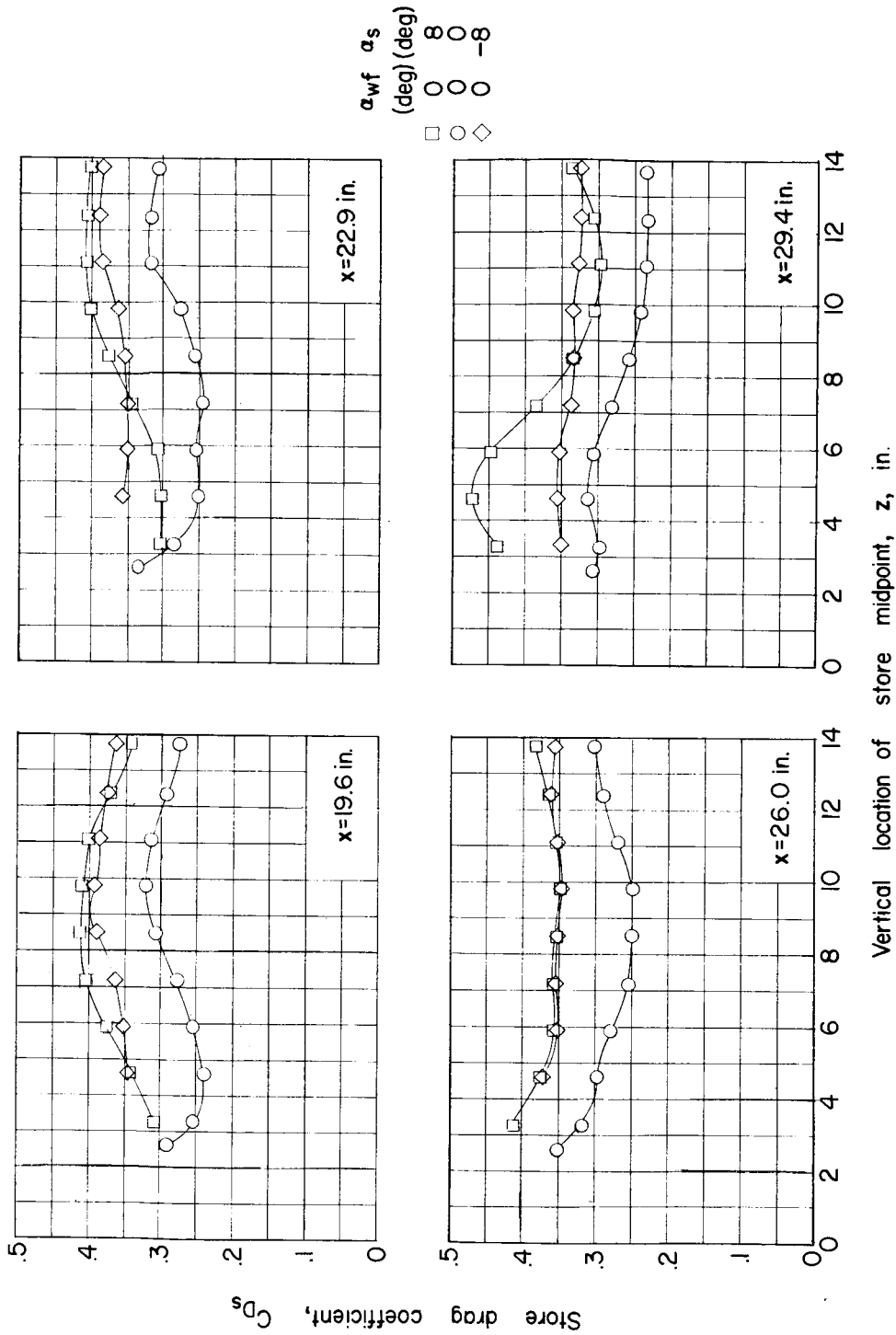


Figure 2.- Aerodynamic characteristics of the isolated store.

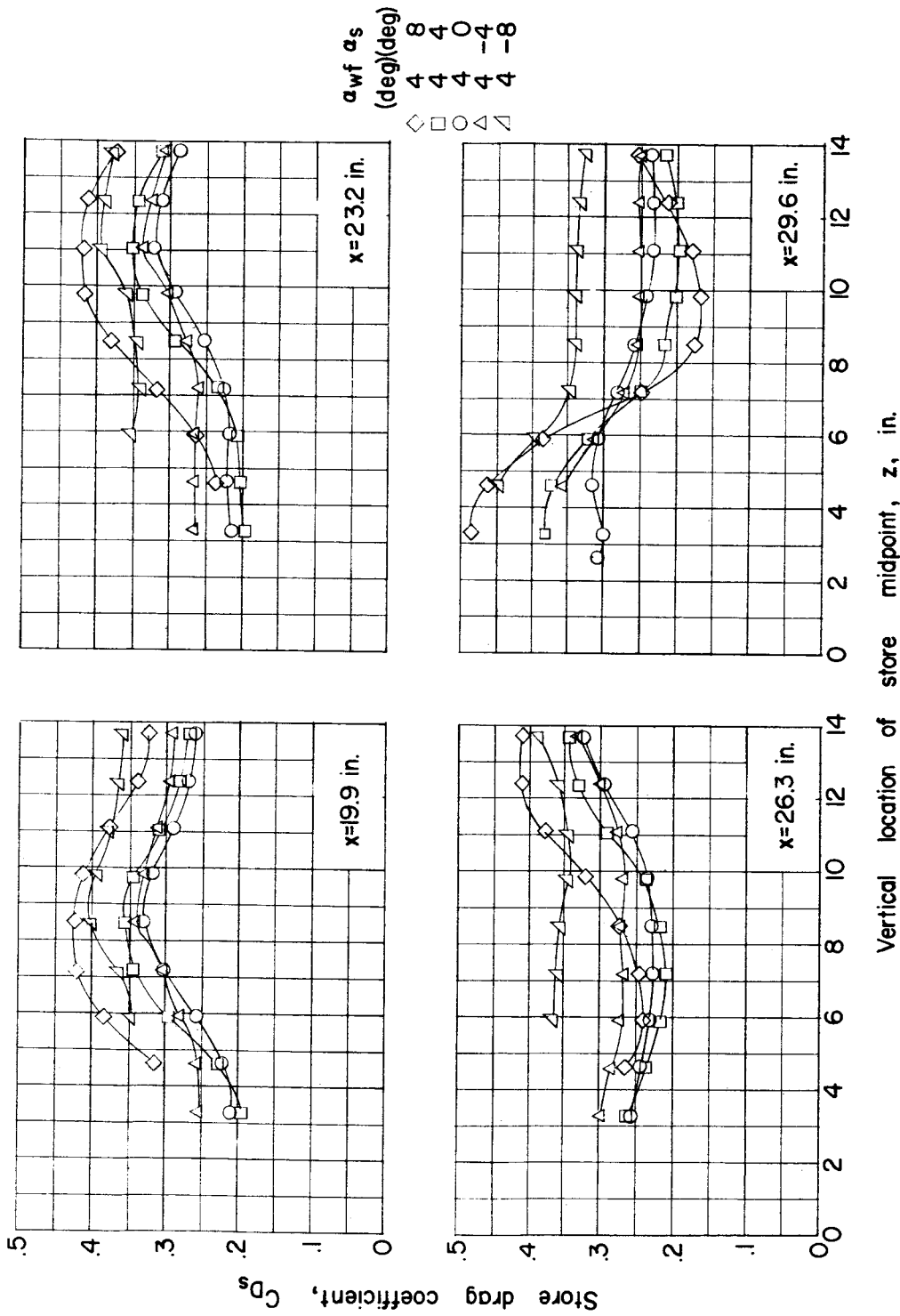




(a)  $\alpha_{wF} = 0^\circ$ .

Figure 3.- Store drag coefficient in the presence of the wing-fuselage combination for various angles of attack and store chordwise locations.

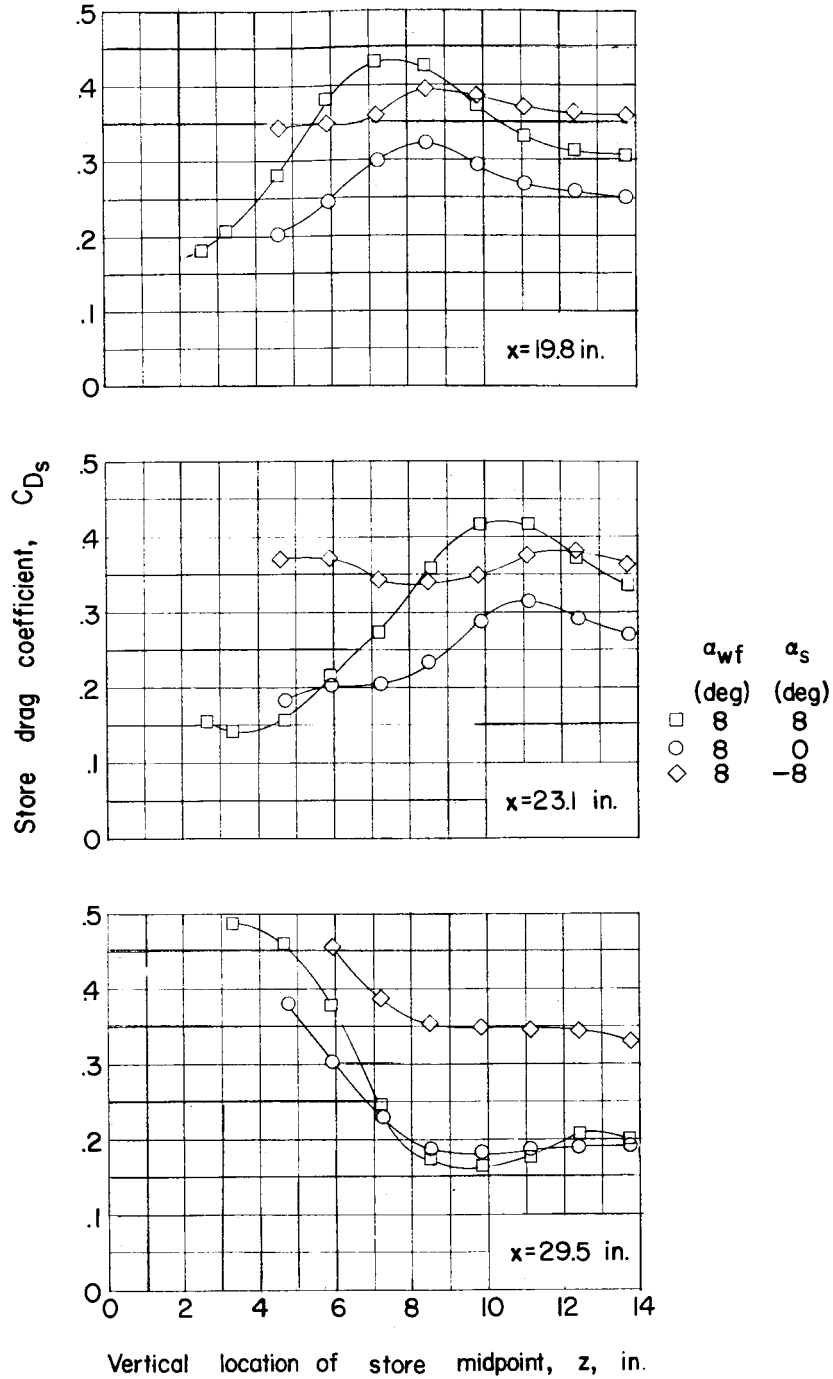




(b)  $\alpha_{wf} = 4^\circ$ .

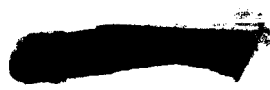
Figure 3.- Continued.

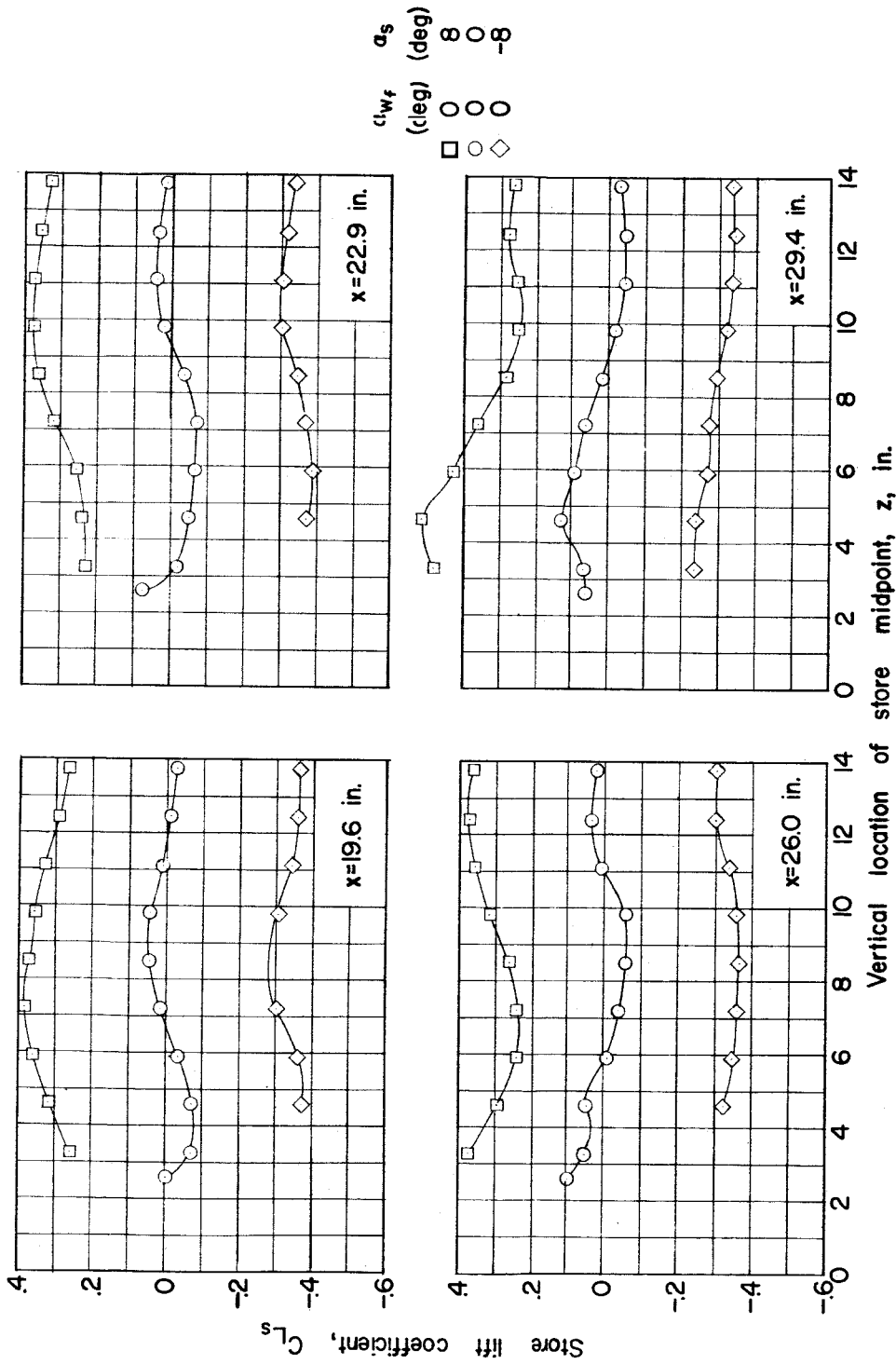




(c)  $\alpha_{wf} = 8^\circ$ .

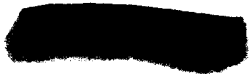
Figure 3.- Concluded.

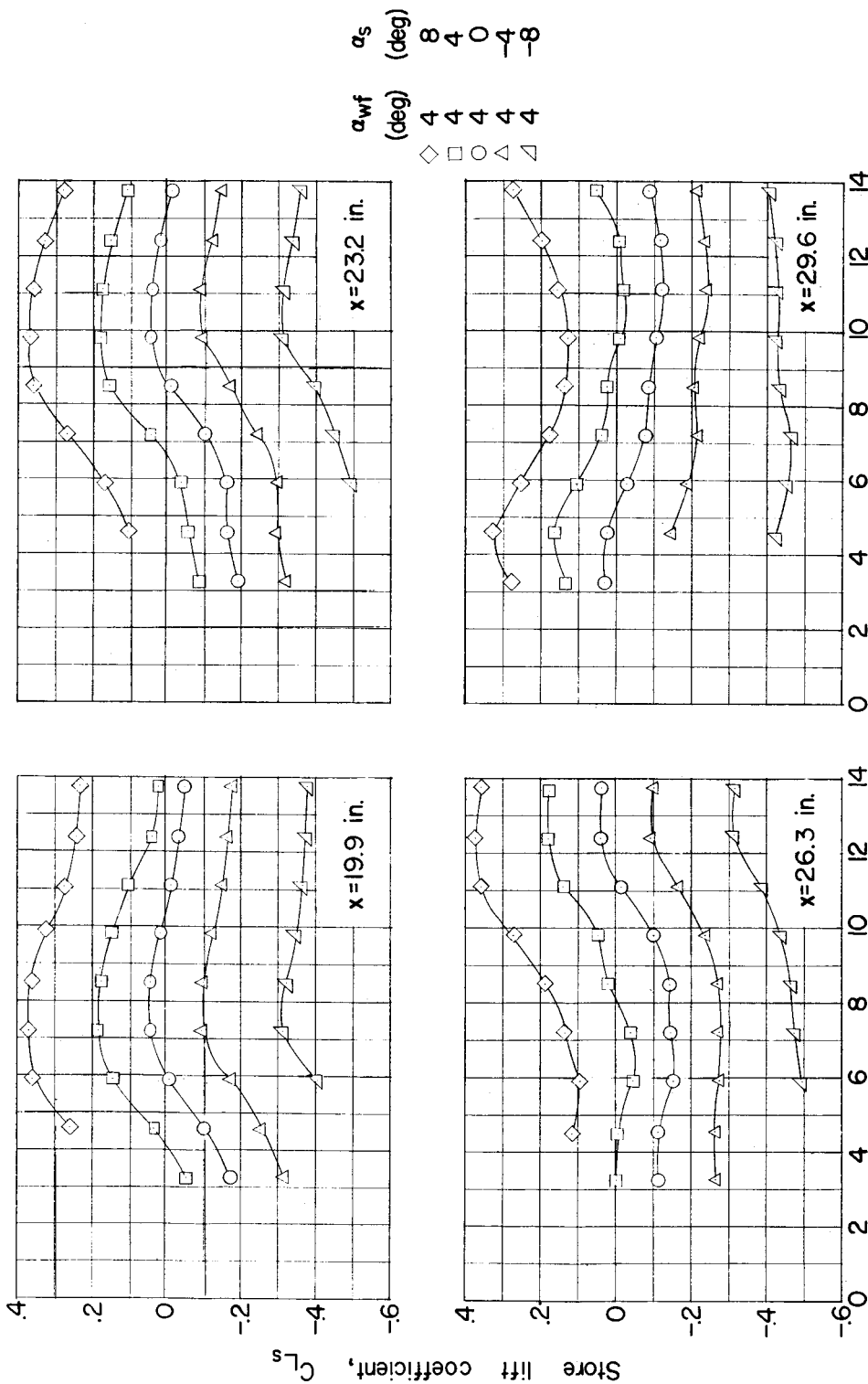




(a)  $\alpha_{wf} = 0^\circ$ .

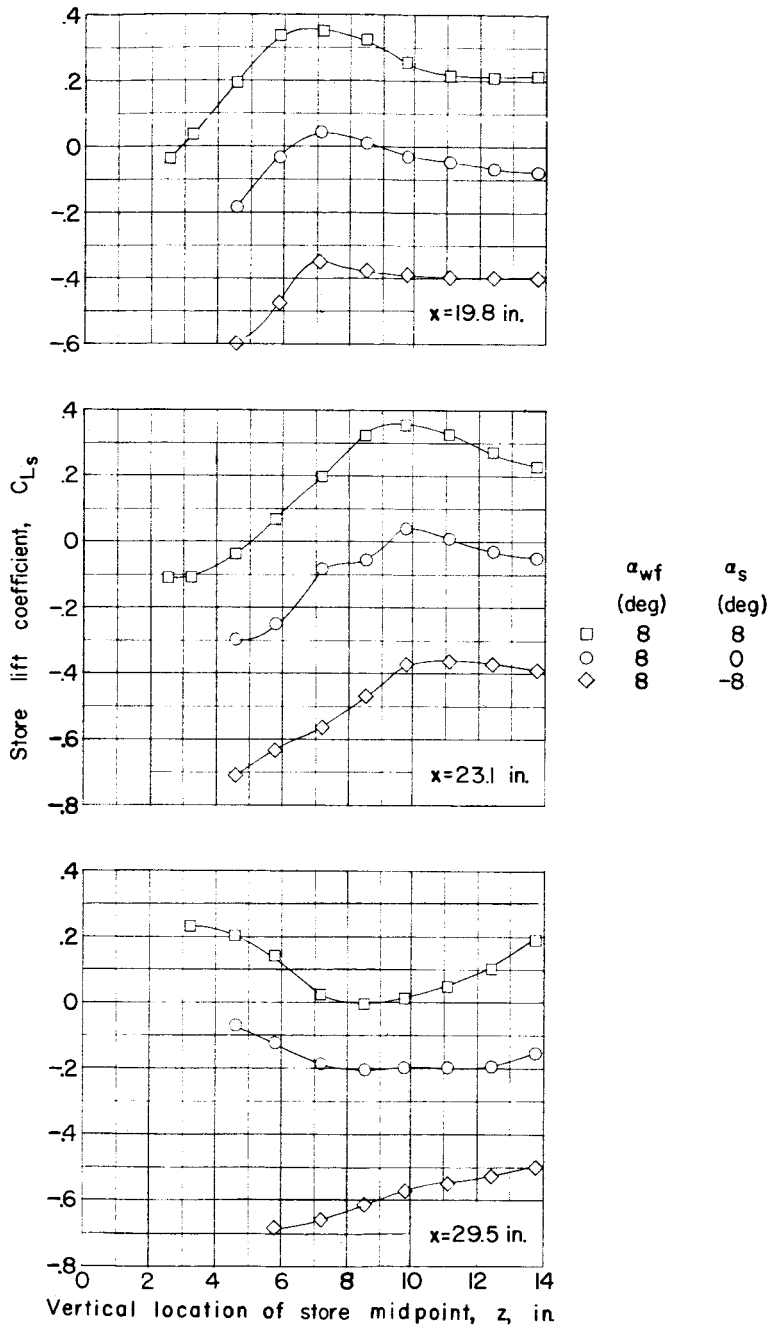
Figure 4.- Store lift coefficient in the presence of the wing-fuselage combination for various angles of attack and store chordwise locations.





(b)  $\alpha_{wf} = 4^\circ$ .

Figure 4.- Continued.



(c)  $\alpha_{wf} = 8^\circ$ .

Figure 4.- Concluded.

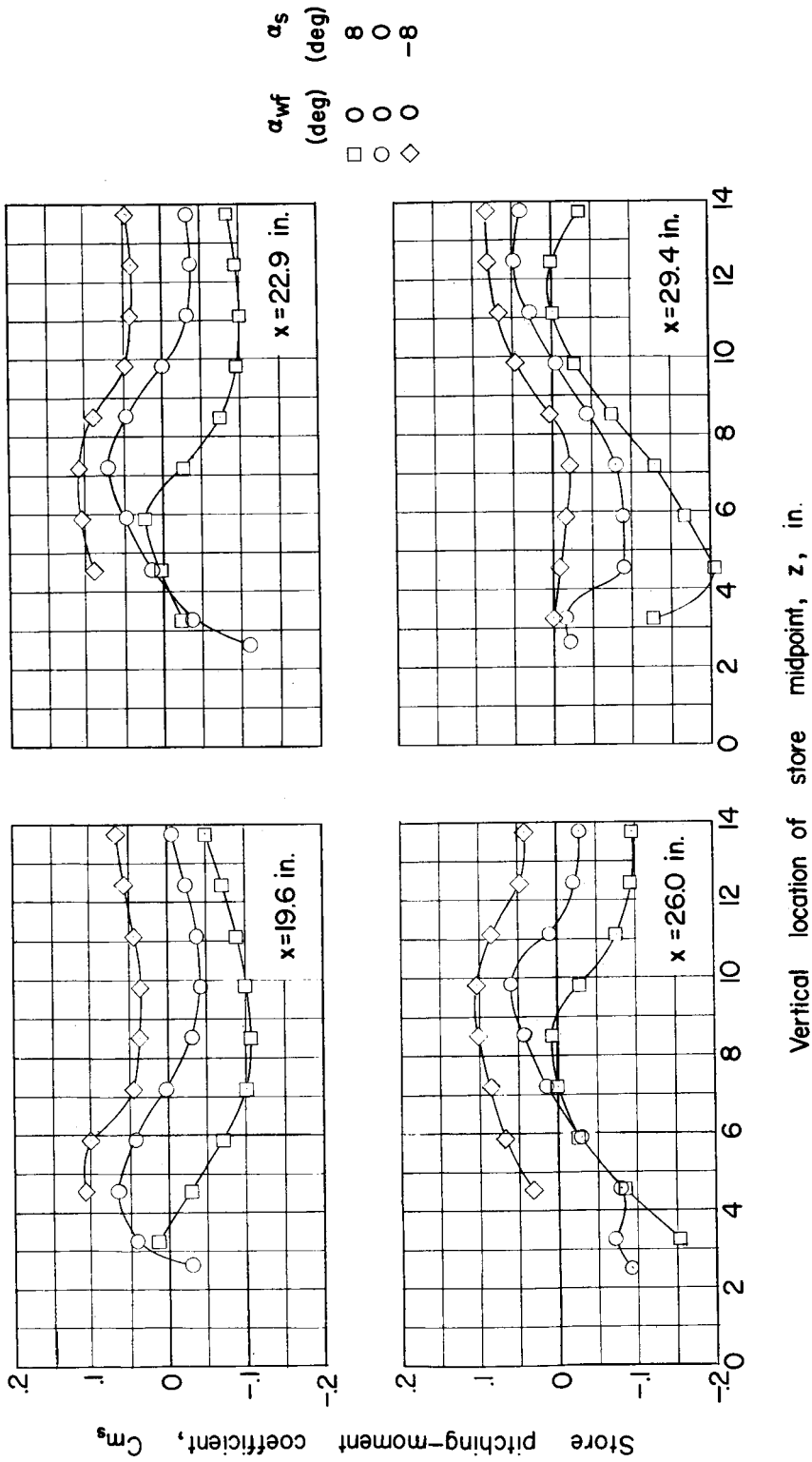
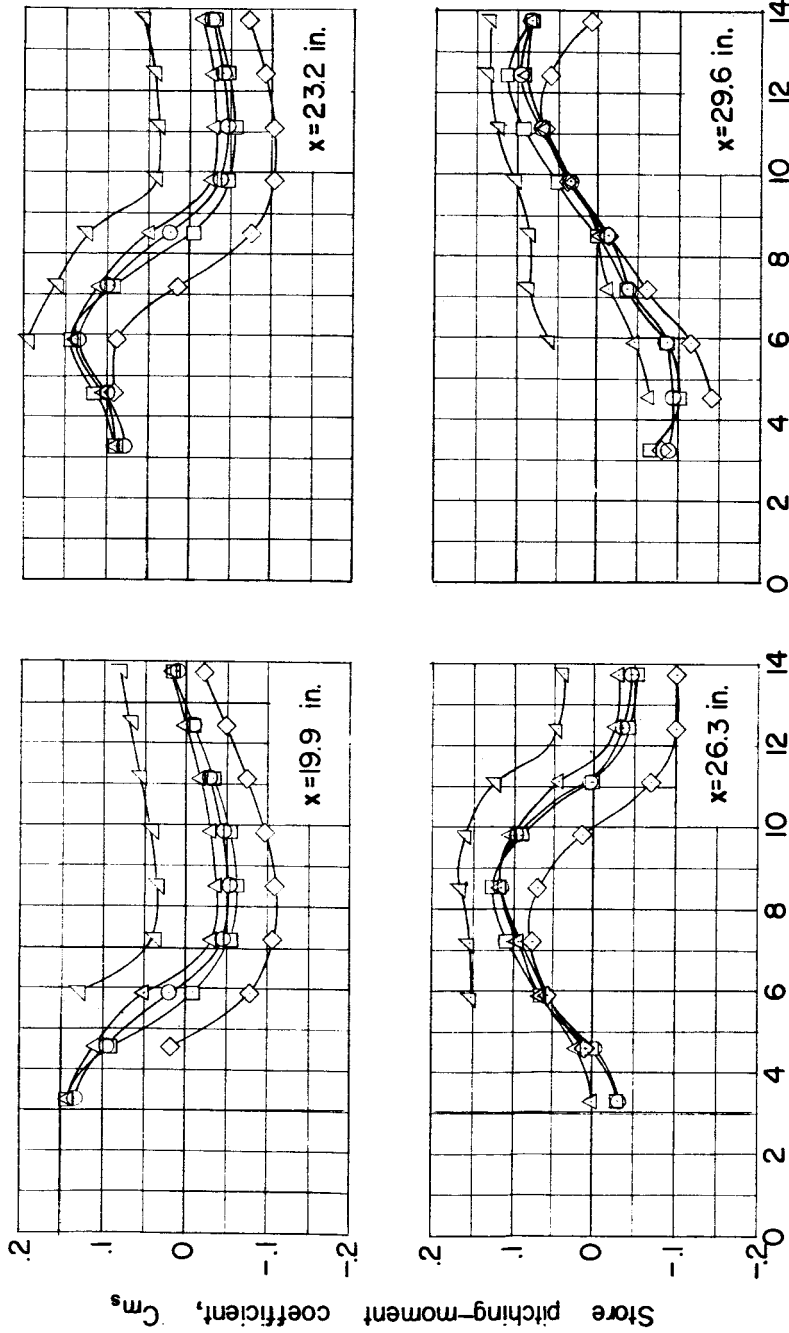


Figure 5.- Store pitching-moment coefficient in the presence of the wing-fuselage combination for various angles of attack and store chordwise locations.

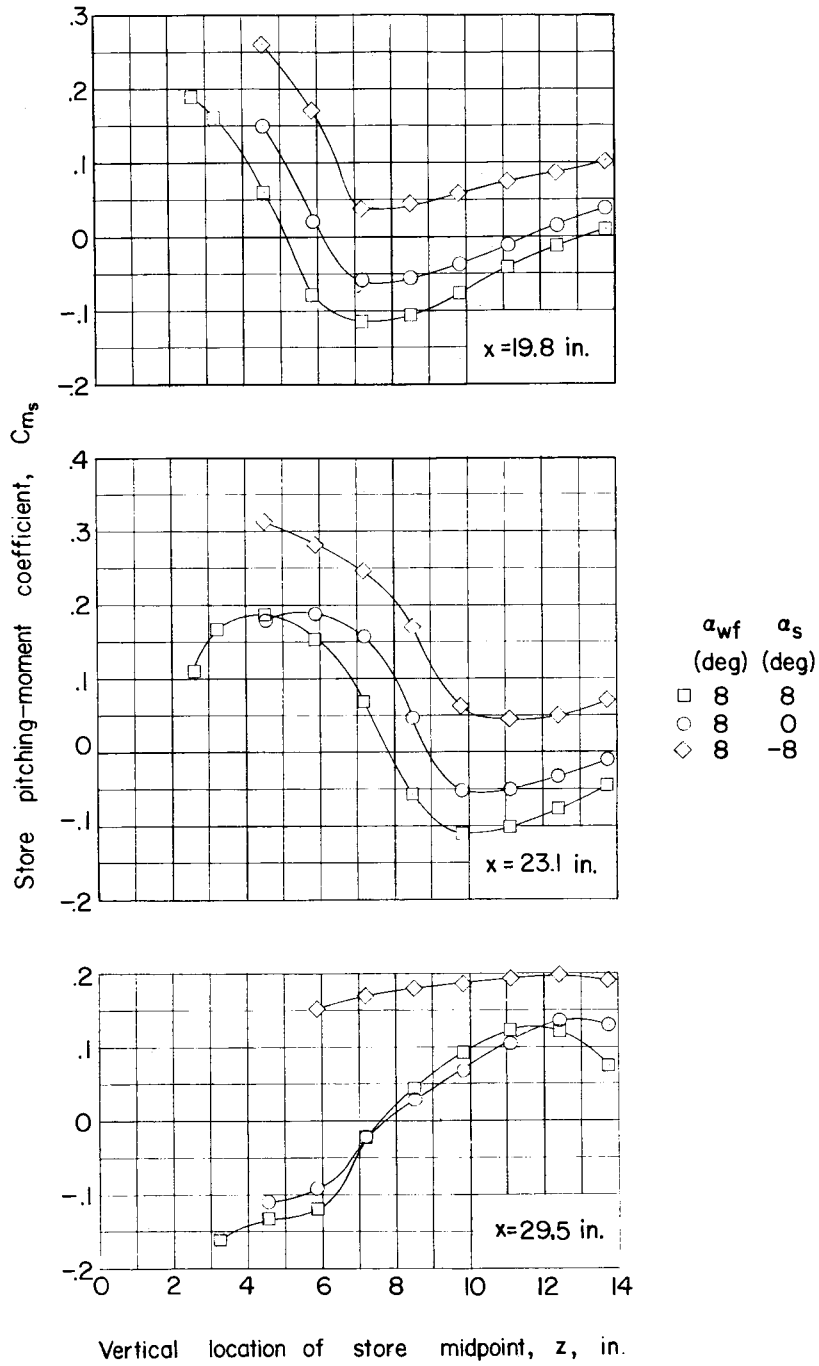


$\alpha_{wf}$  (deg)    4   4   4   4   4  
 $\alpha_s$  (deg)     8   4   4   -4   8  
 ◇   □   ○   △   ▽



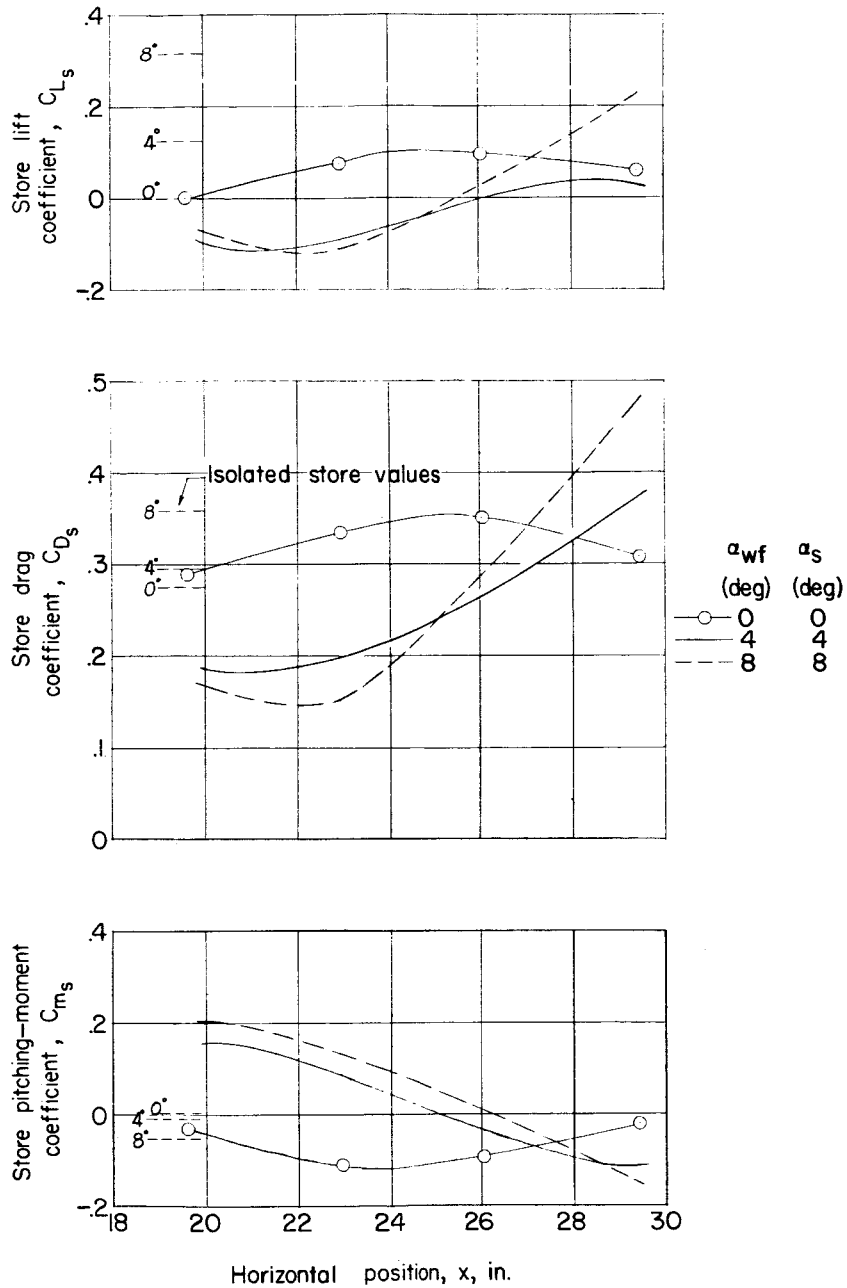
(b)  $\alpha_{wf} = 4^\circ$ .

Figure 5.- Continued.



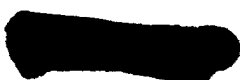
(c)  $\alpha_{wf} = 8^\circ$ .

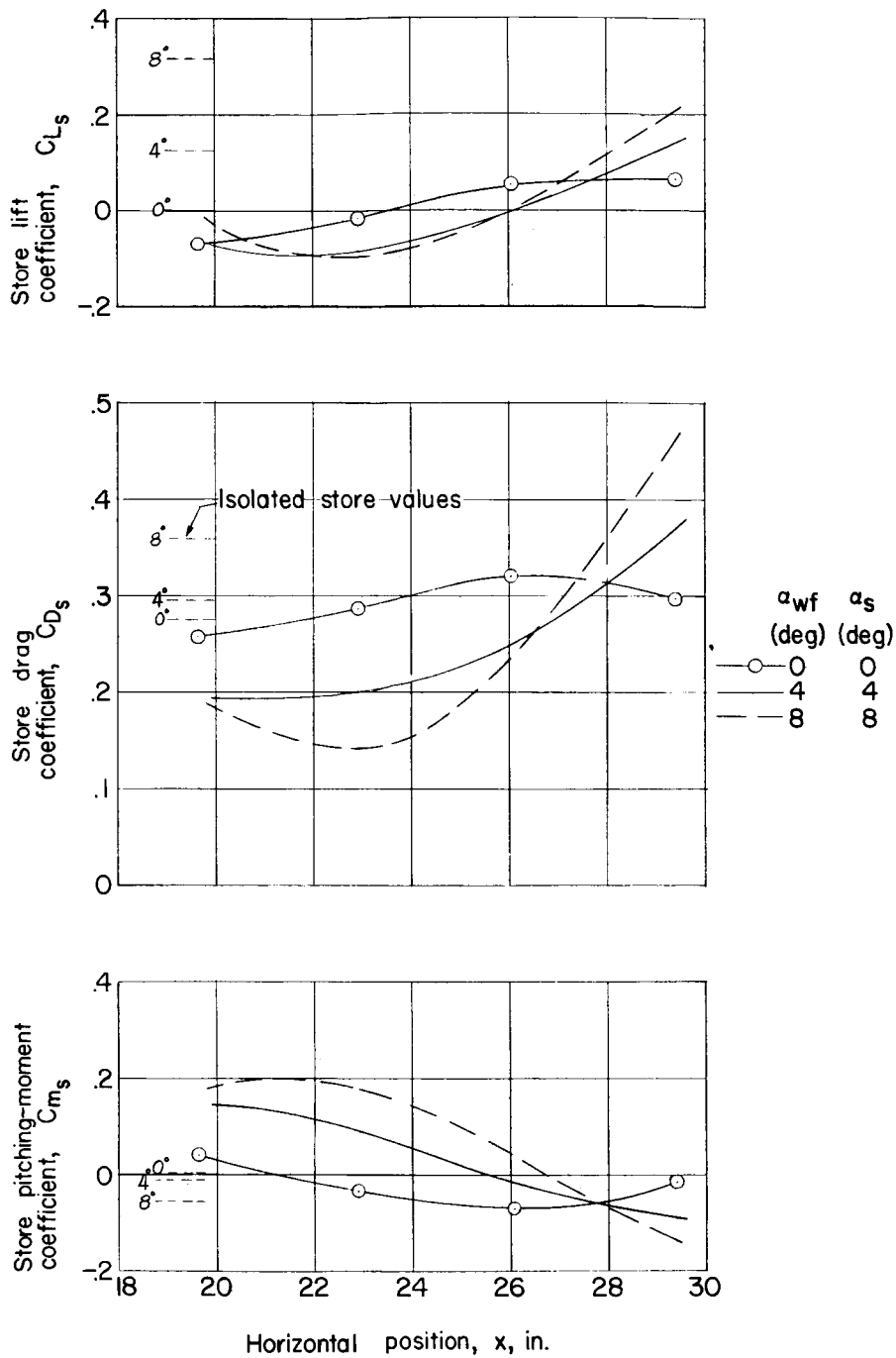
Figure 5.- Concluded.



(a)  $h' = 1.12$  inches.

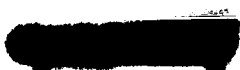
Figure 6.- Variation of store lift, drag, and pitching-moment coefficient with store horizontal position in presence of wing-fuselage combination;  $\alpha_{wf} = \alpha_s$ .

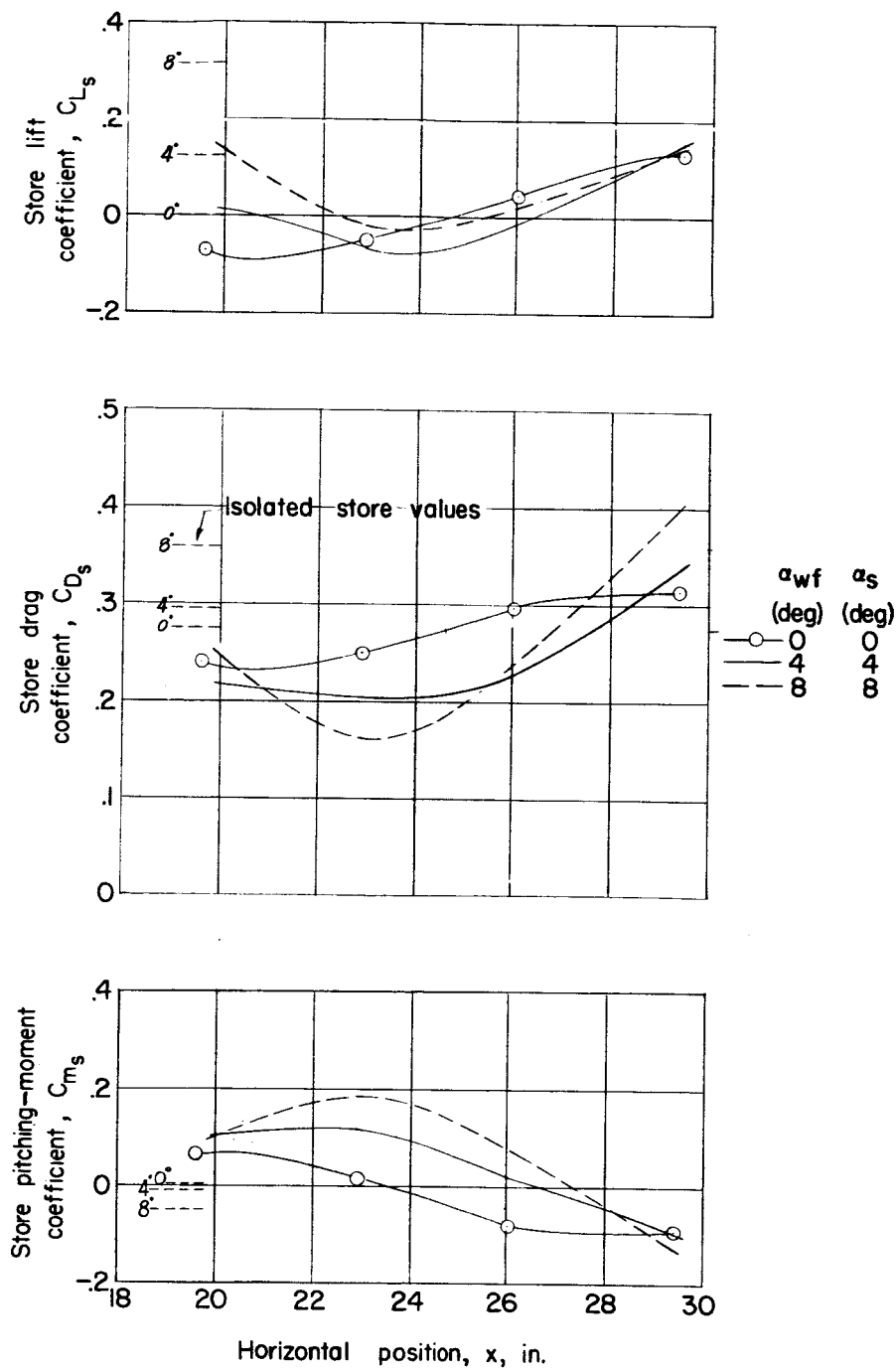




(b)  $h' = 1.77$  inches.

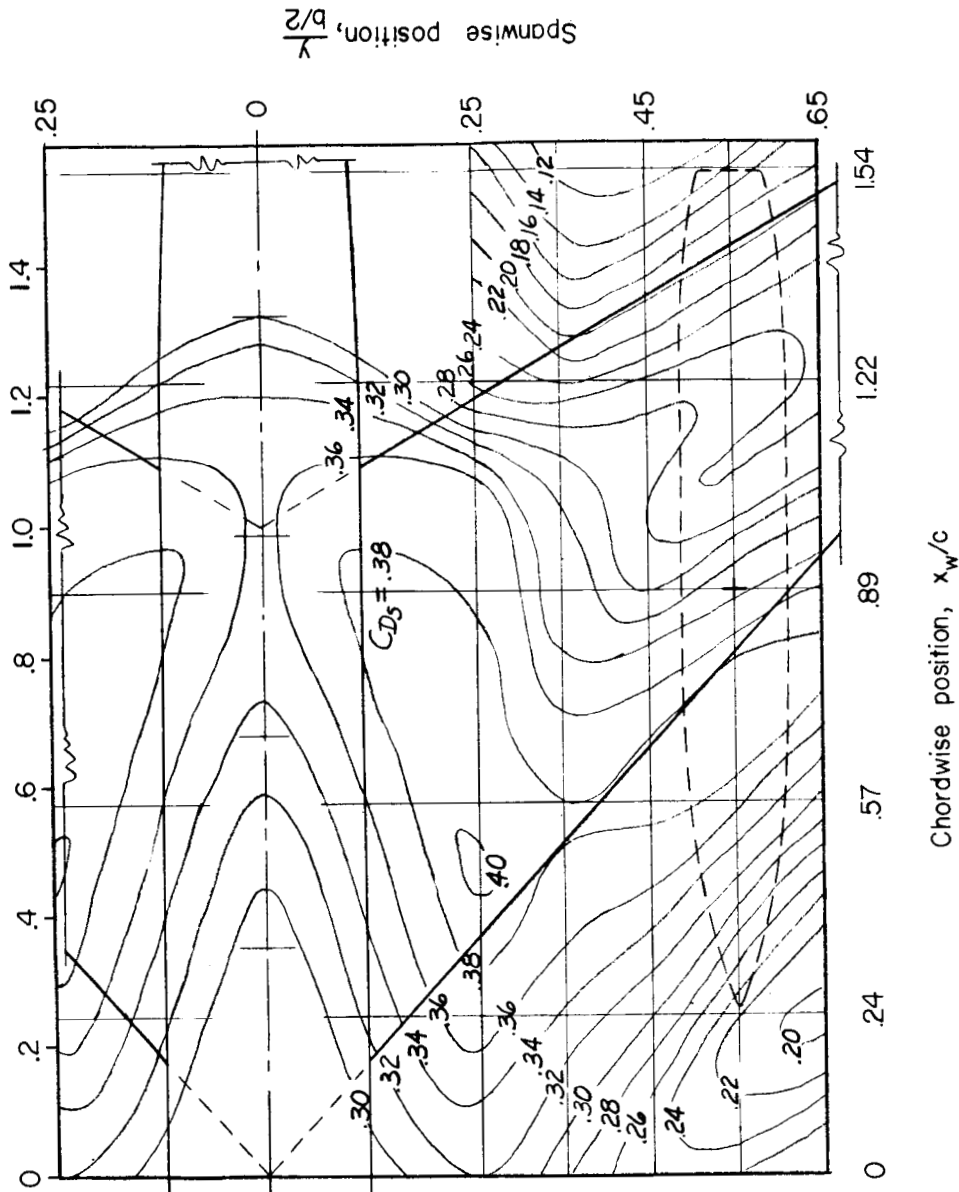
Figure 6.- Continued.



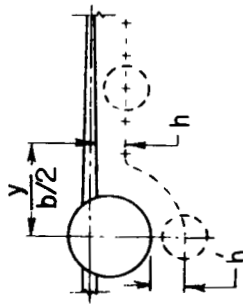


(c)  $h' = 3.08$  inches.

Figure 6.- Concluded.

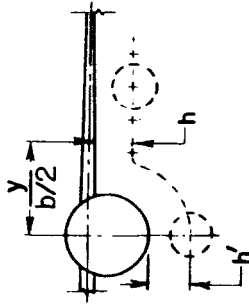
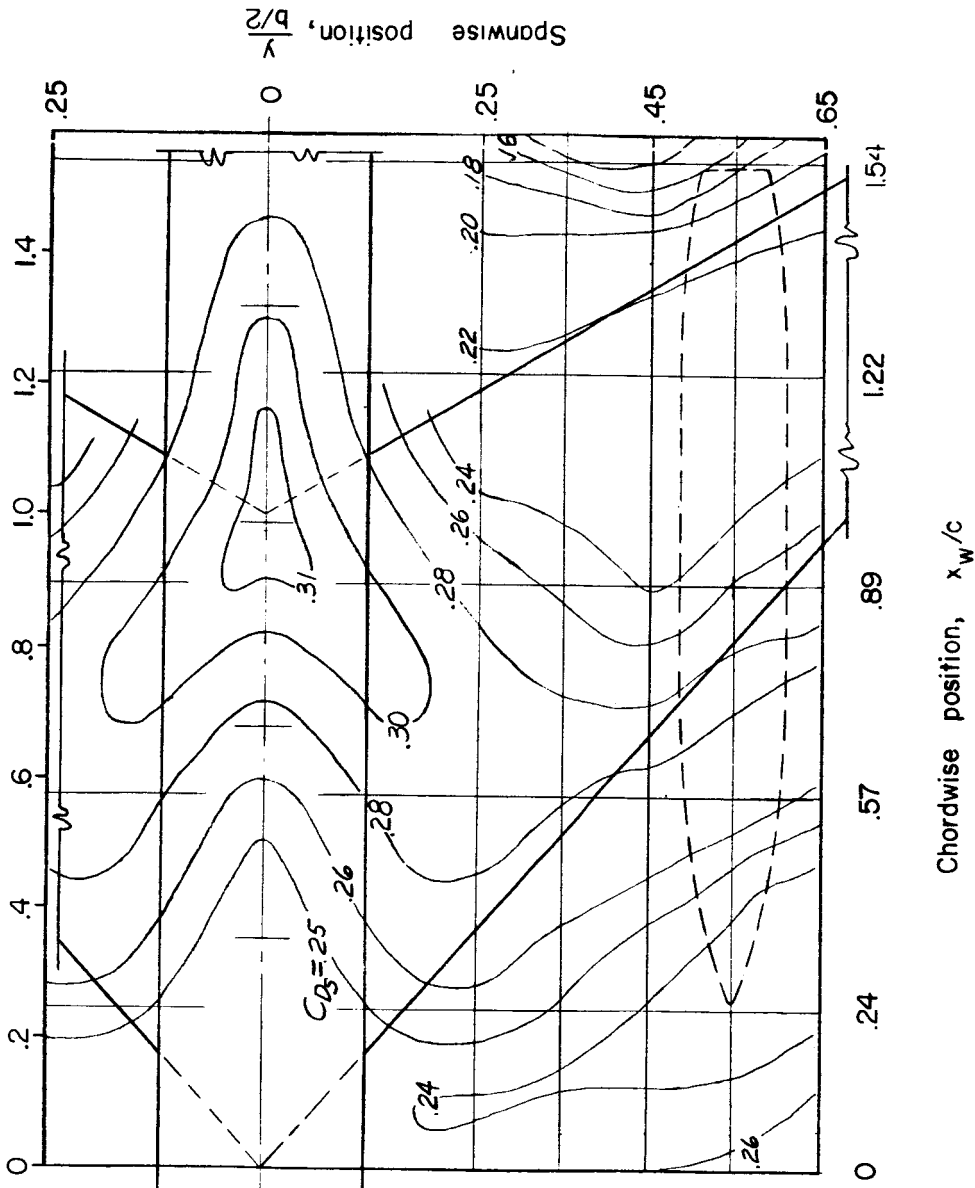


(a)  $h'/d = 0.68$ ;  $\alpha = 0^\circ$ ; isolated  $C_{D_s} = 0.275$ .



$\frac{h'}{d} = .68 \left( \frac{y}{b/2} = 0 \right)$   
 $\frac{h'}{d} = .62 \left( \frac{y}{b/2} = .25 \right)$   
 $(z = 1.15 \text{ in., ref II})$

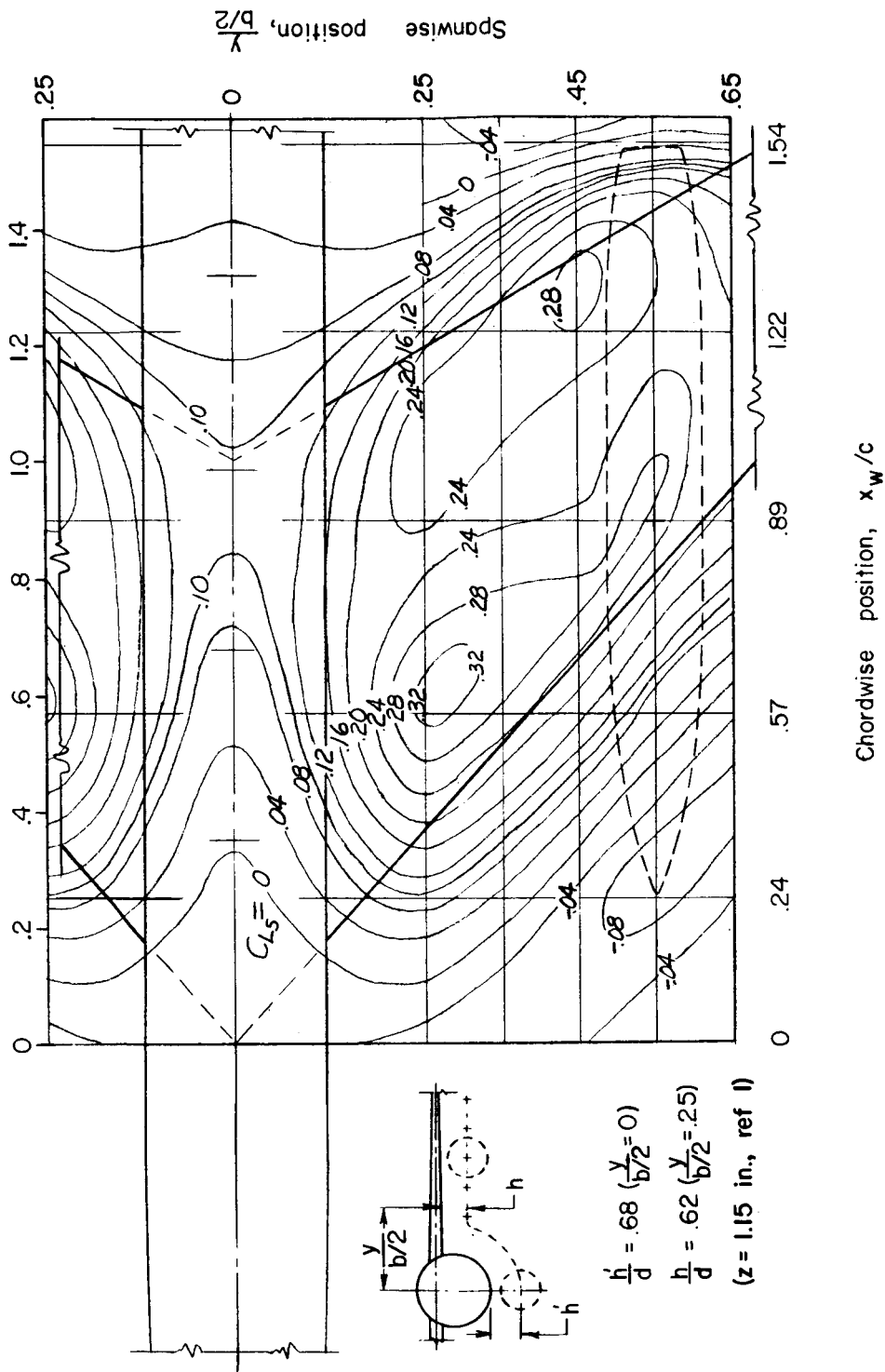
Figure 7.- Spanwise contour plot of store drag coefficient in the presence of the wing-fuselage combination. (Wing contour data from ref. 1.)



$\frac{h}{d} = 1.24 \left( \frac{y}{b/2} = 0 \right)$   
 $\frac{h}{d} = 1.24 \left( \frac{y}{b/2} = .25 \right)$   
 (z = 2.09 in., ref 1)

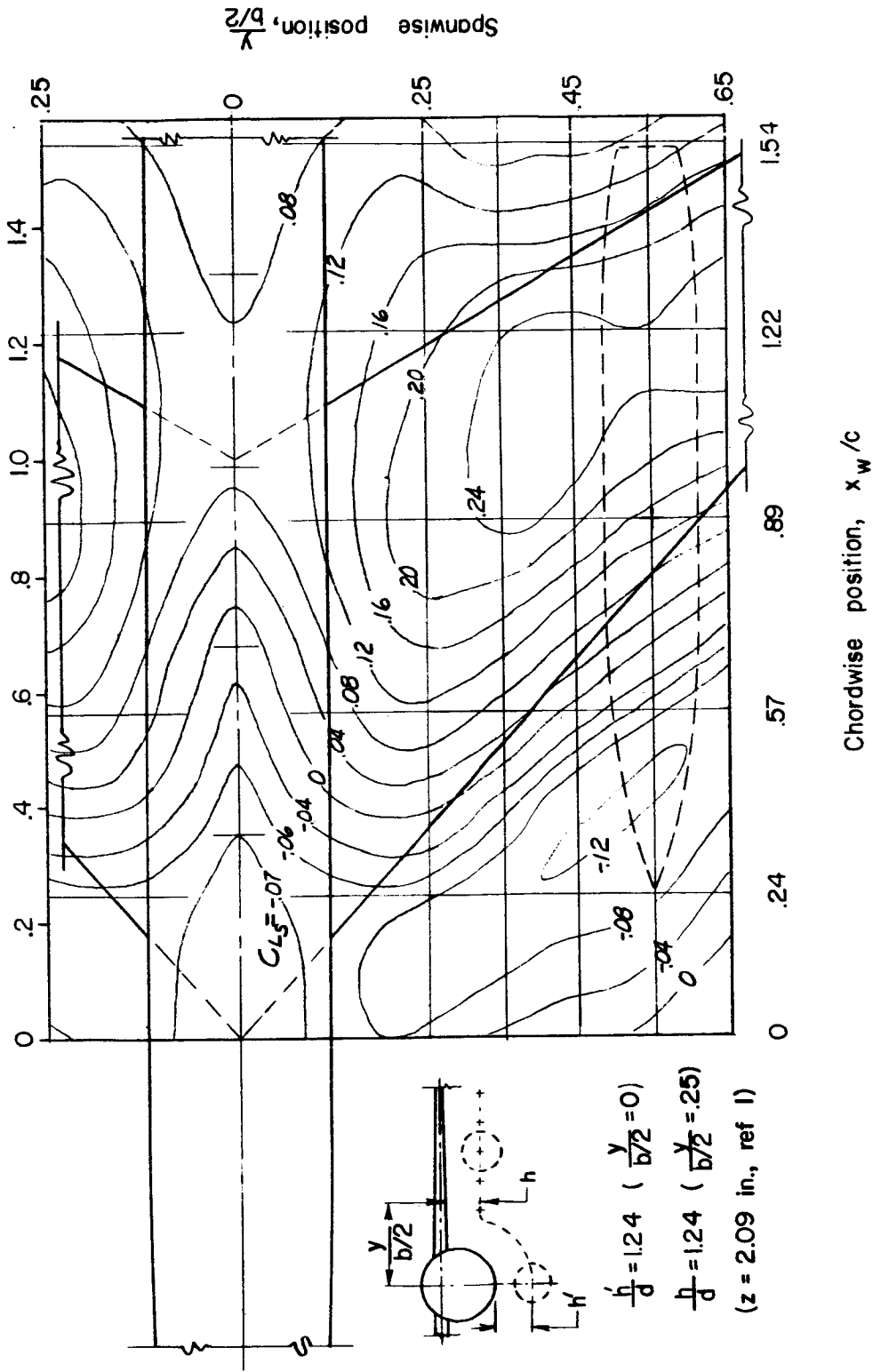
(b)  $h'/d = 1.24$ ;  $\alpha = 0^\circ$ ; isolated  $C_{D_s} = 0.275$ .

Figure 7.- Concluded.



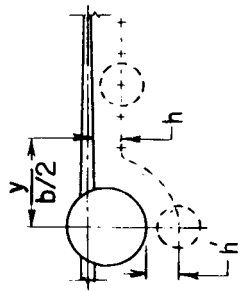
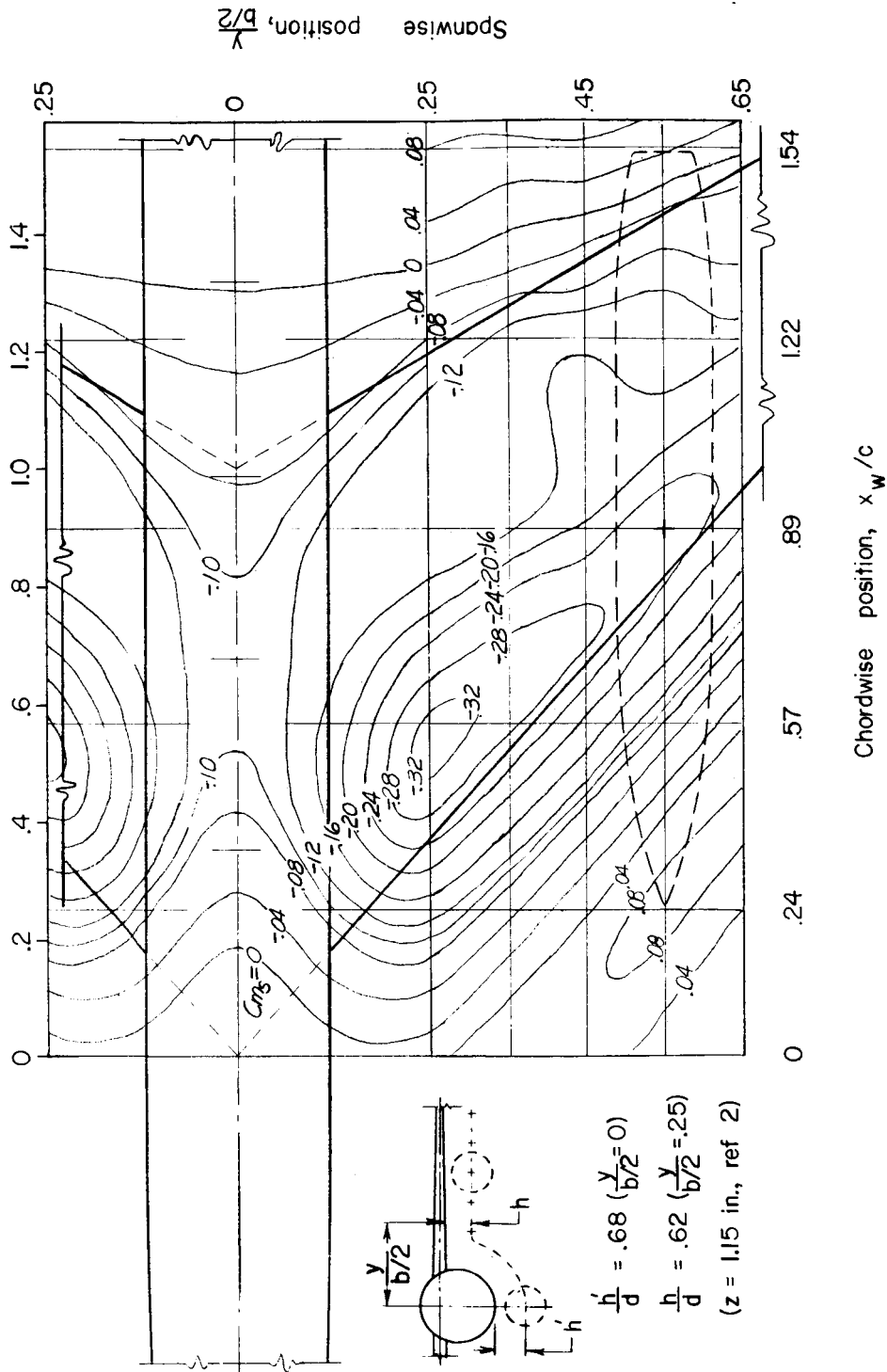
(a)  $h'/d = 0.68$ ;  $\alpha = 0^\circ$ ; isolated  $C_{L_s} = 0$ .

Figure 8.- Spanwise contour plot of store lift coefficient in the presence of the wing-fuselage combination. (Wing contour data from ref. 2.)

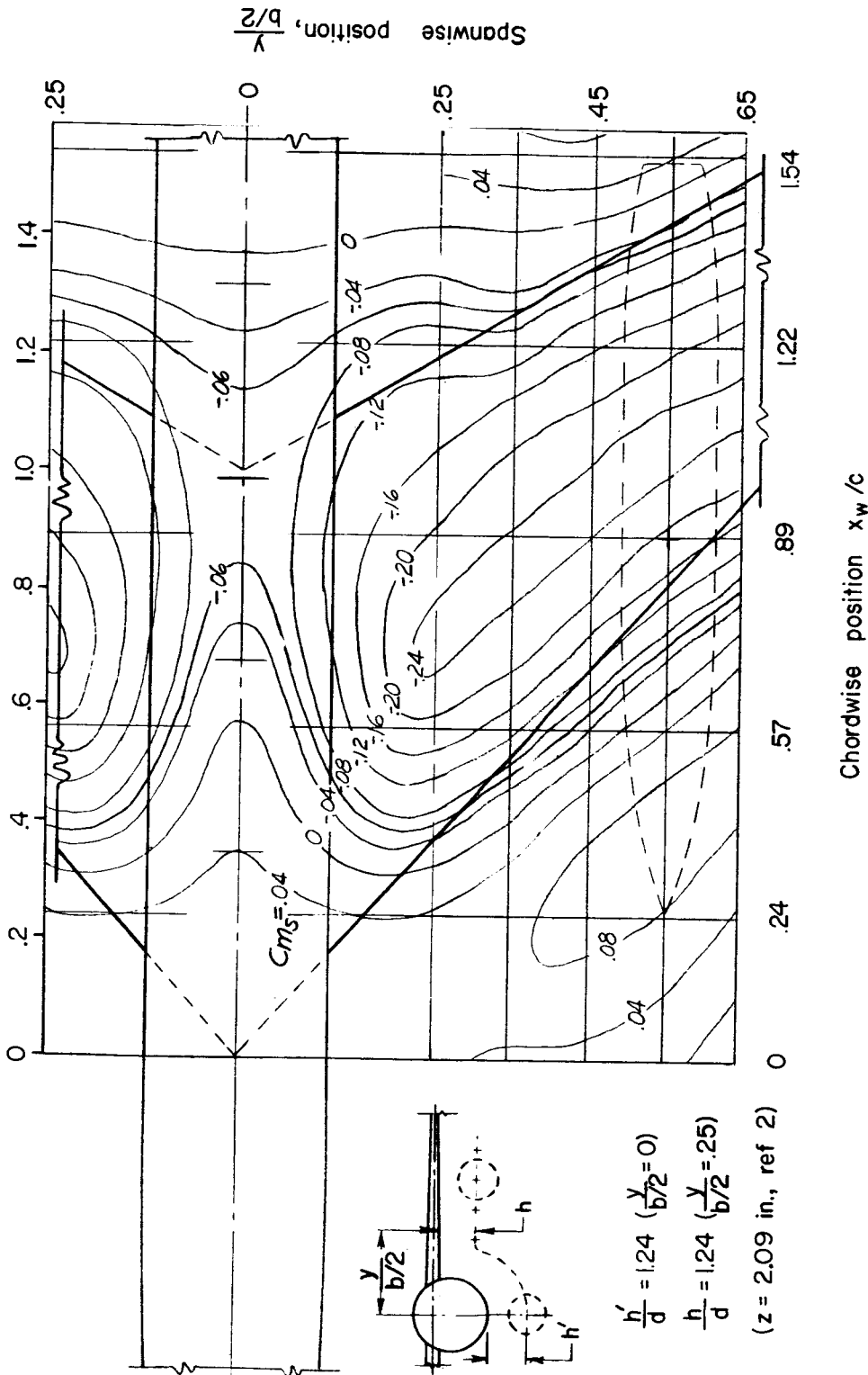


(b)  $h'/d = 1.24$ ;  $\alpha = 0^\circ$ ; isolated  $C_{I_{16}} = 0$ .

Figure 8.- Concluded.

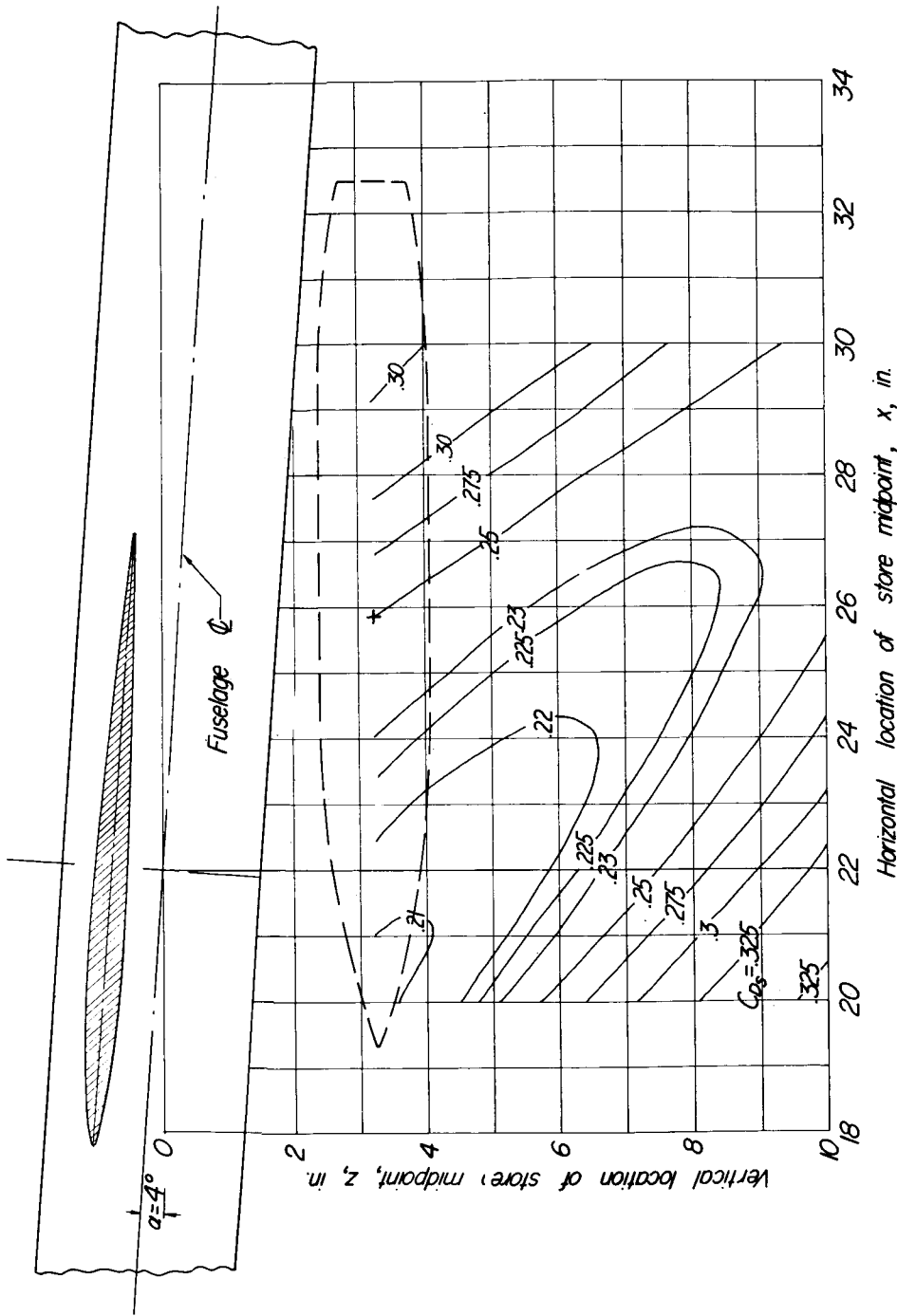


$\frac{h}{d} = 0.68 \left( \frac{y}{b/2} = 0 \right)$   
 $\frac{h}{d} = 0.62 \left( \frac{y}{b/2} = 0.25 \right)$   
 $(z = 1.15 \text{ in., ref 2})$



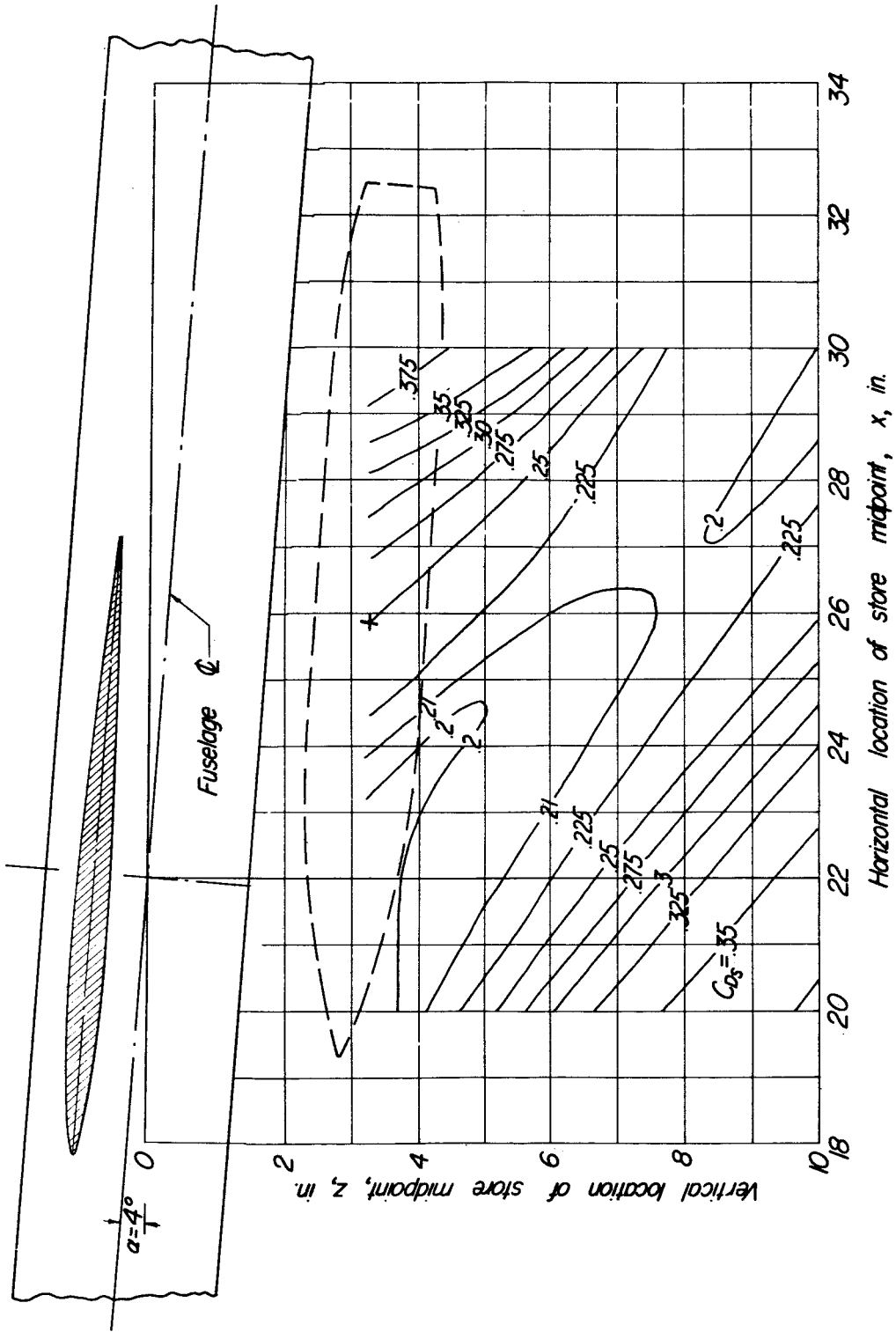
(b)  $h'/d = 1.24$ ;  $\alpha = 0^\circ$ ; isolated  $C_{mS} = 0$ .

Figure 9.- Concluded.



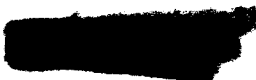
(a)  $\alpha_{wf} = 4^\circ$ ;  $\alpha_s = 0^\circ$ .

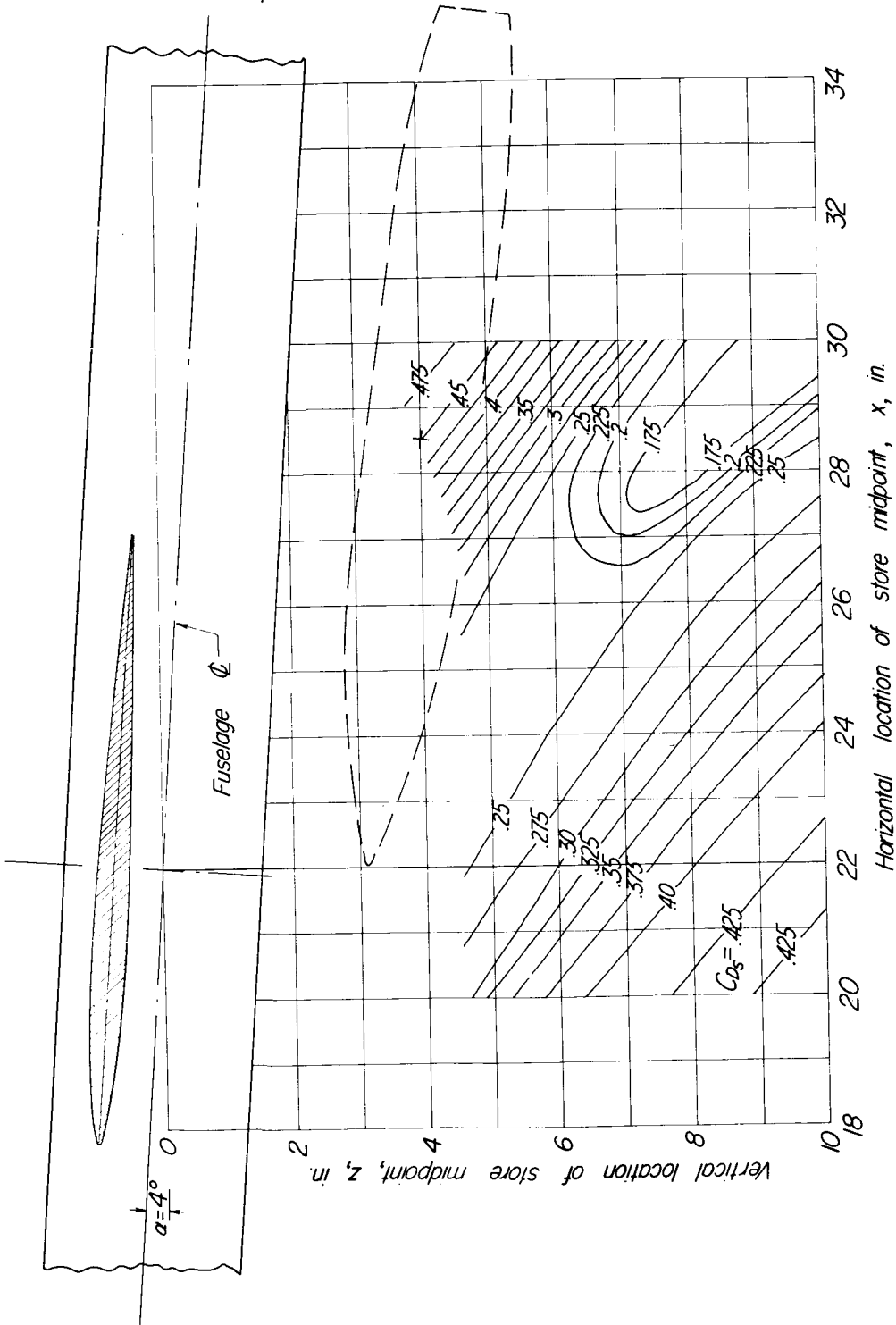
Figure 10.-- Vertical contour plot of store drag coefficient in presence of wing-fuselage combination. (Wing section shown at fuselage surface.)



(b)  $\alpha_{wF} = 4^\circ$ ;  $\alpha_{ES} = 4^\circ$ .

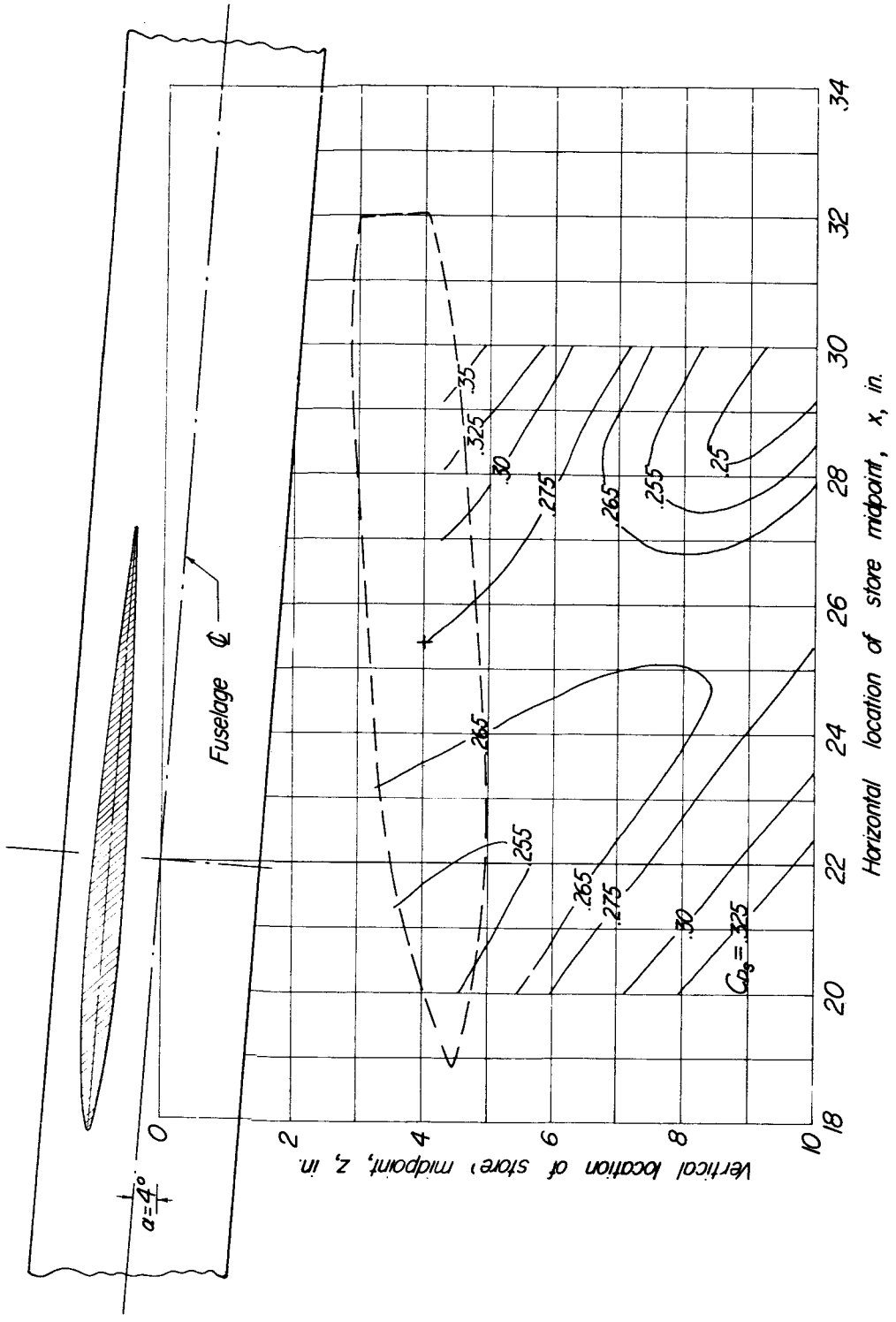
Figure 10.- Continued.





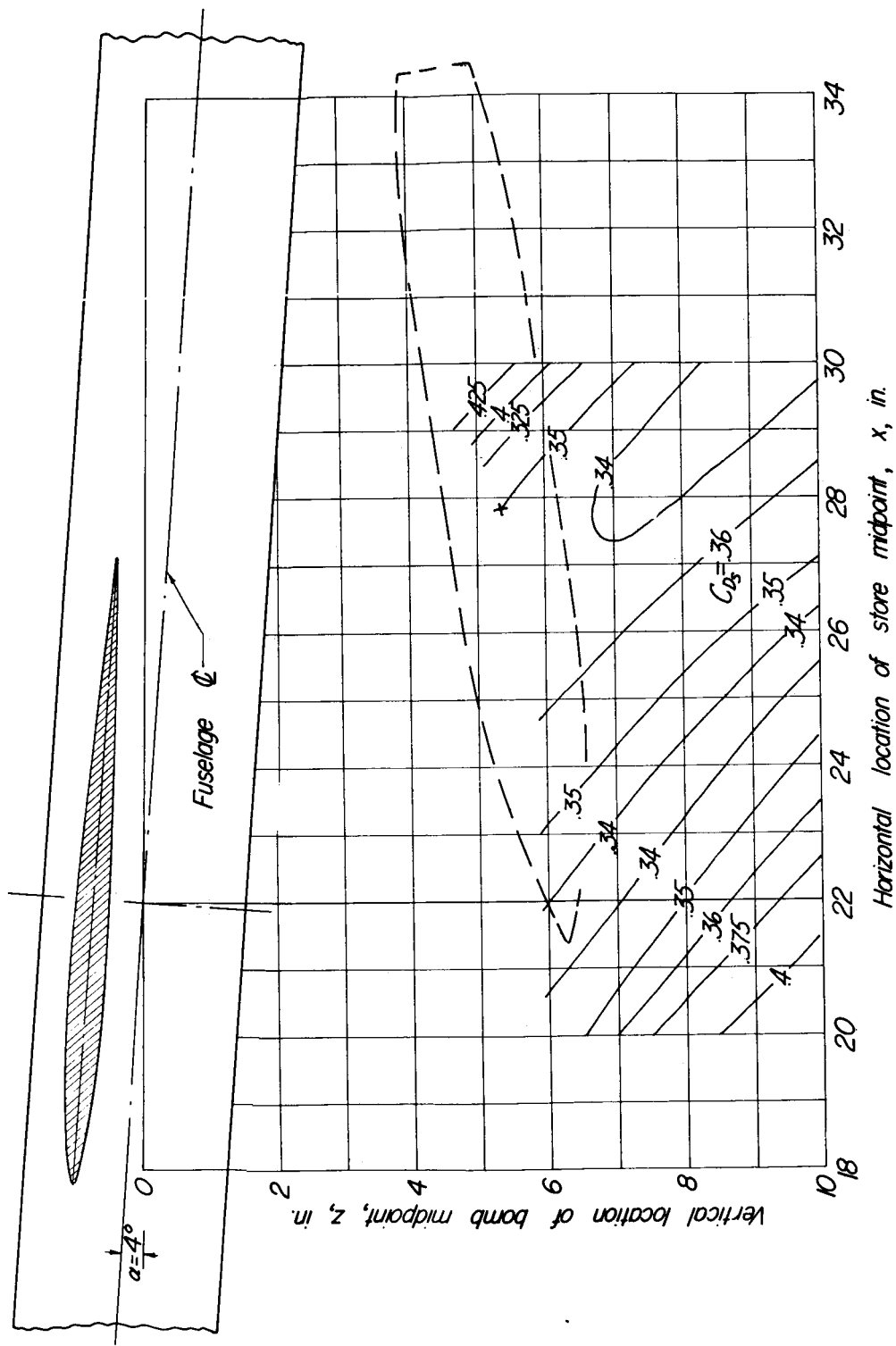
(c)  $\alpha_{wF} = 4^\circ$ ;  $\alpha_S = 8^\circ$ .

Figure 10.- Continued.



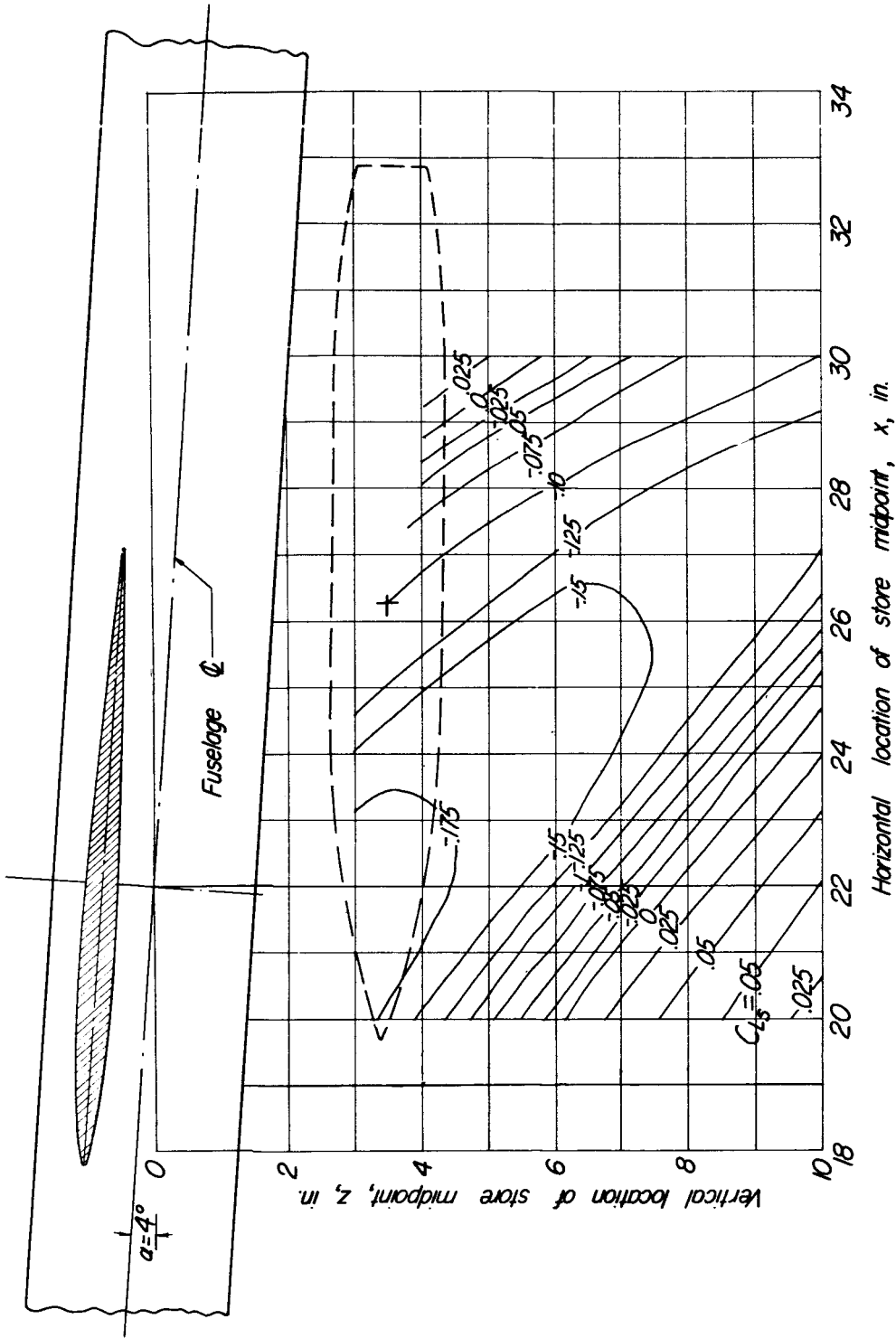
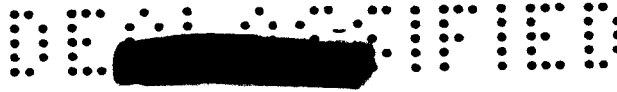
(d)  $\alpha_{WF} = 4^\circ$ ;  $\alpha_S = -4^\circ$ .

Figure 10.- Continued.



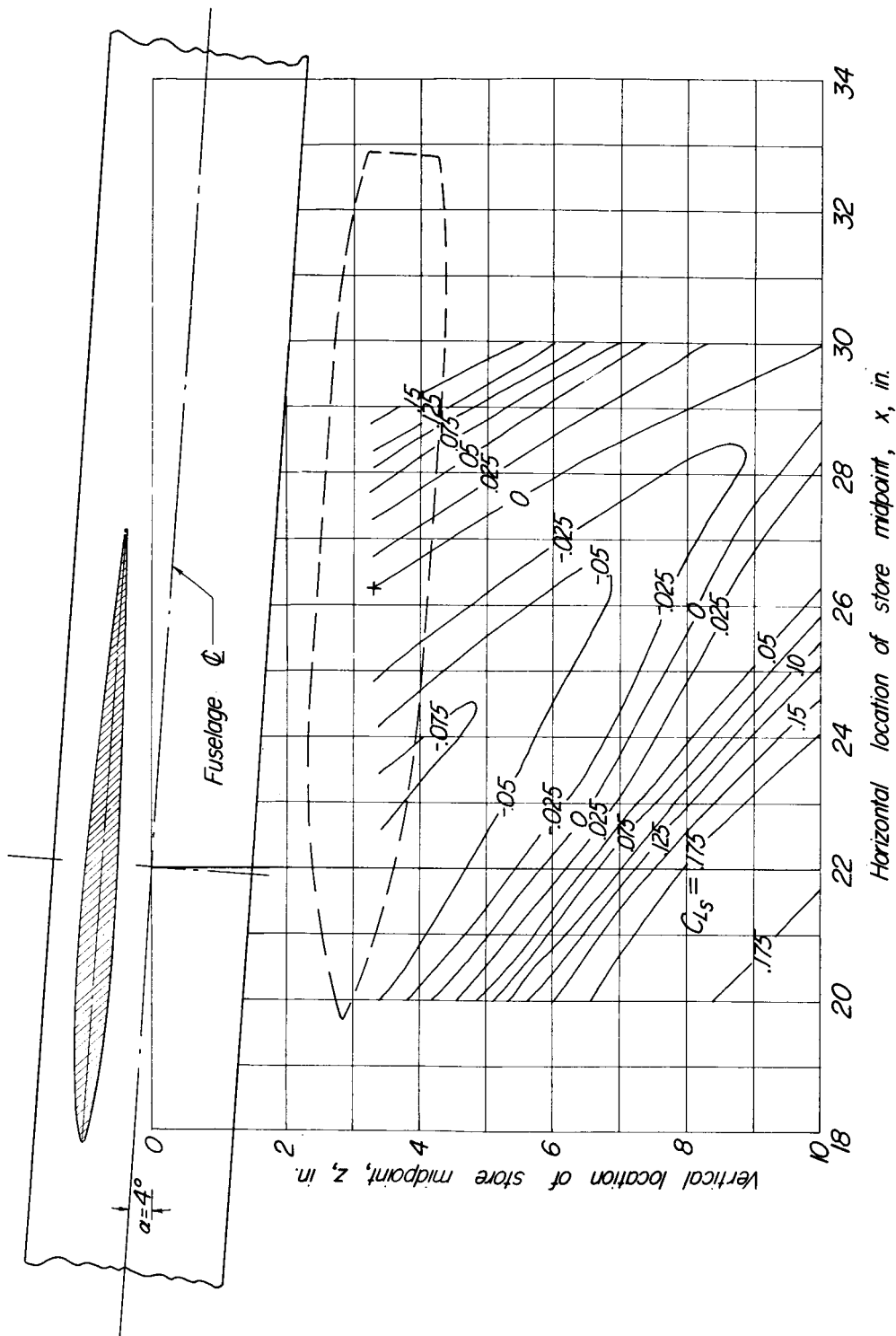
(e)  $\alpha_{wf} = 4^\circ$ ;  $\alpha_s = -8^\circ$ .

Figure 10.- Concluded.



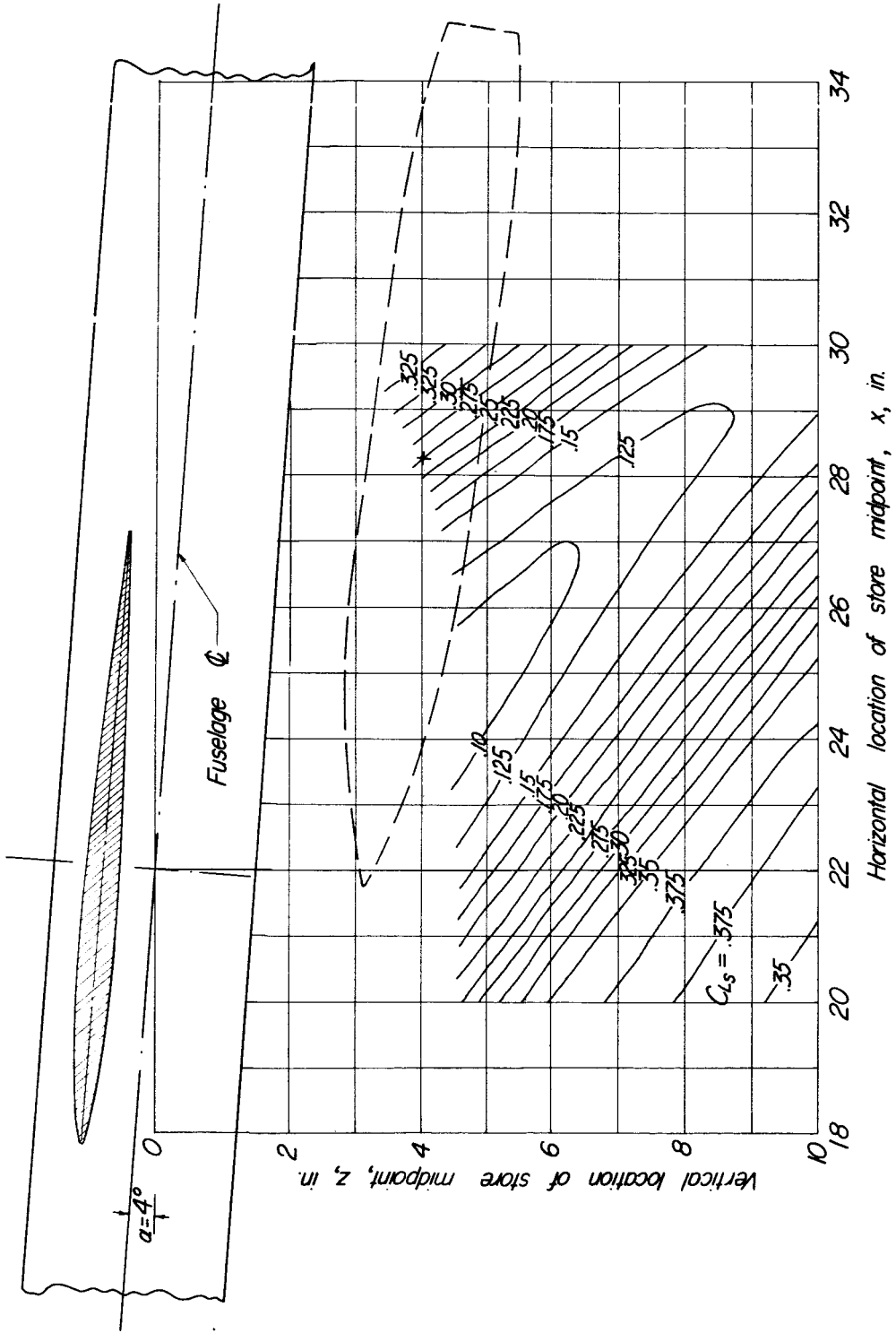
(a)  $\alpha_{wf} = 4^\circ$ ;  $\alpha_g = 0^\circ$ .

Figure 11.- Vertical contour plot of store lift coefficient in presence of wing-fuselage combination. (Wing section shown at fuselage surface.)



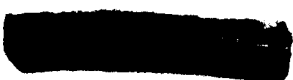
(b)  $\alpha_{wf} = 4^\circ$ ;  $\alpha_s = 4^\circ$ .

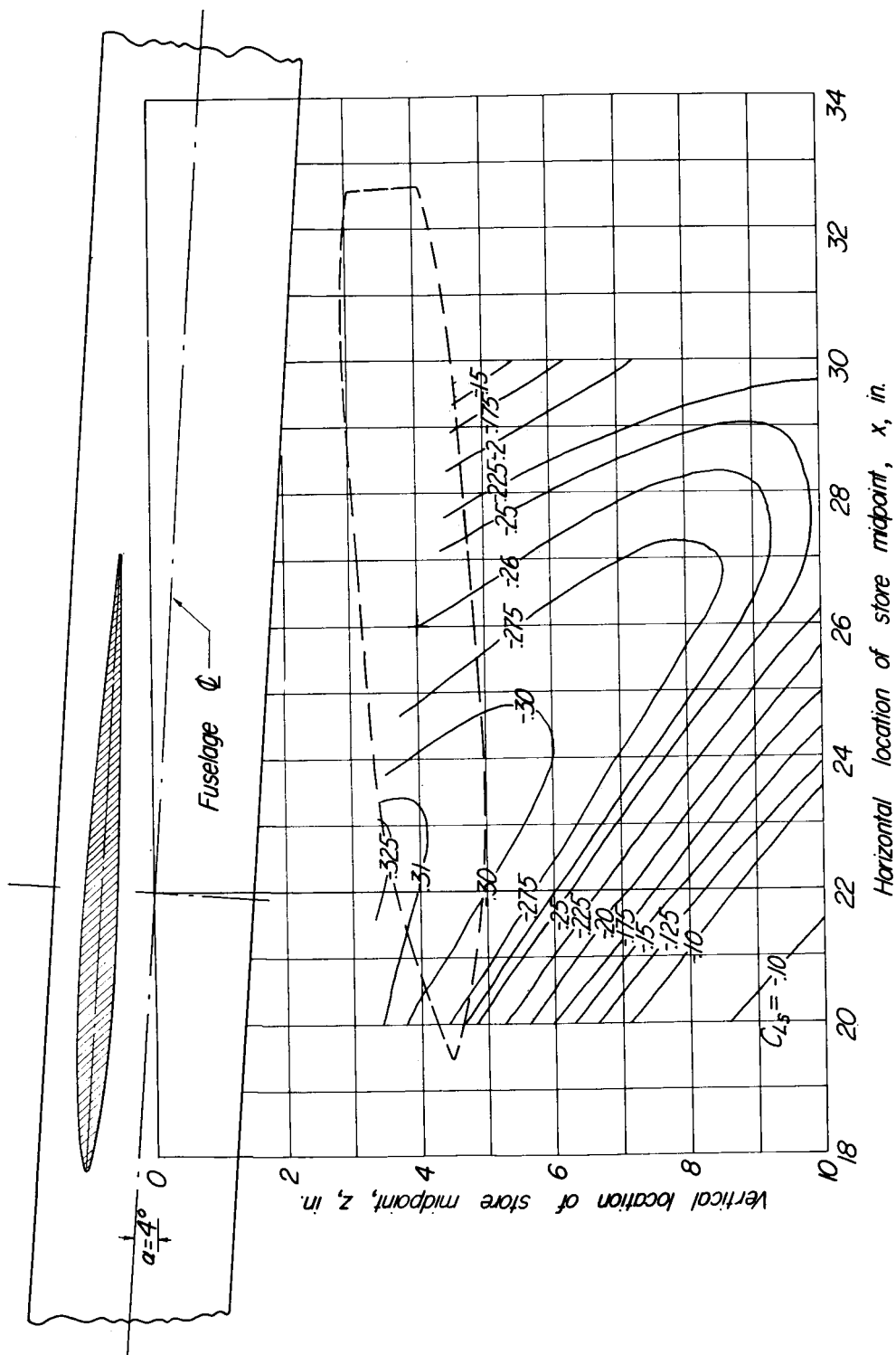
Figure 11.- Continued.



(c)  $\alpha_{WF} = 4^\circ$ ;  $\alpha_g = 8^\circ$ .

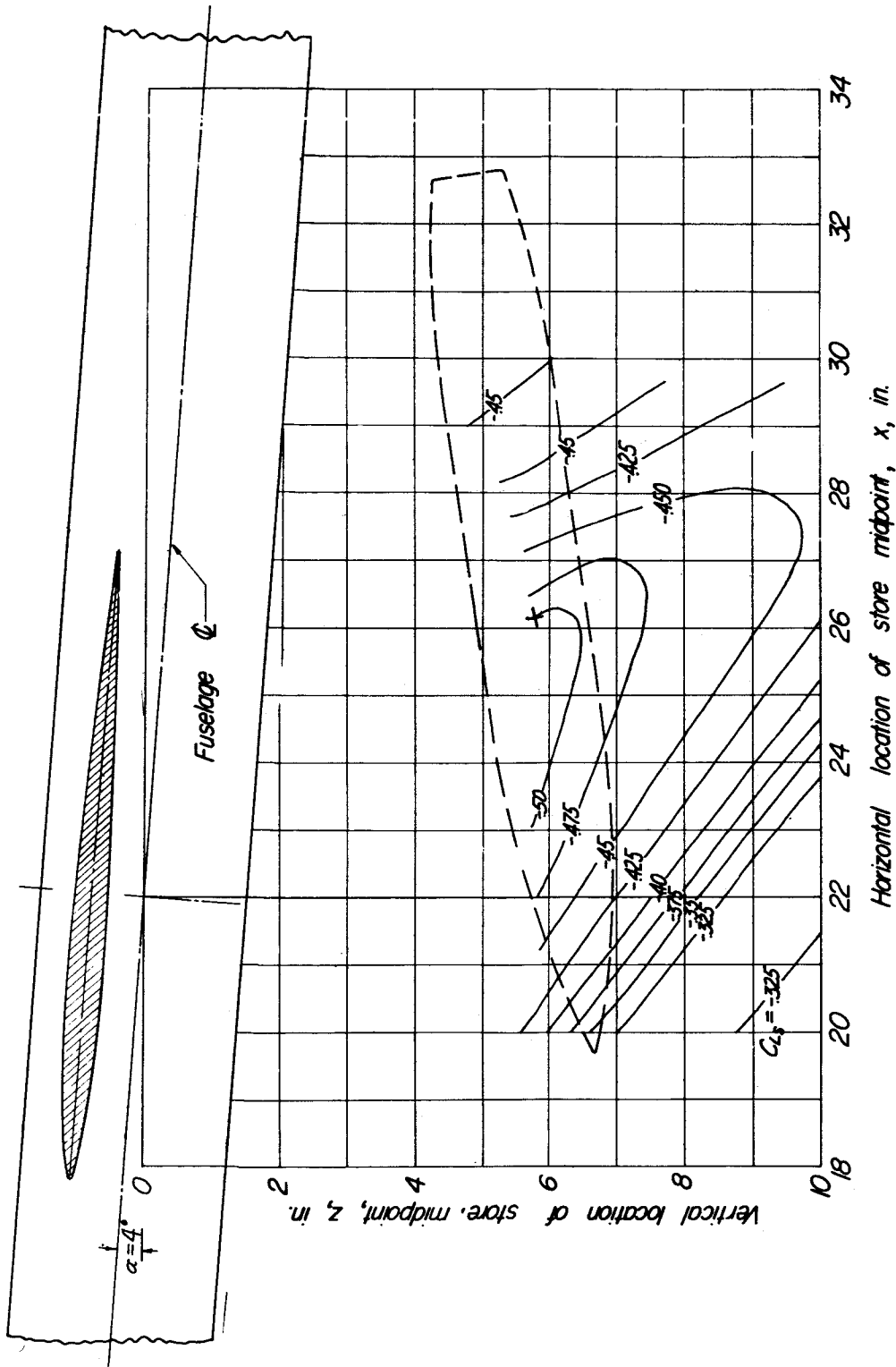
Figure 11.- Continued.





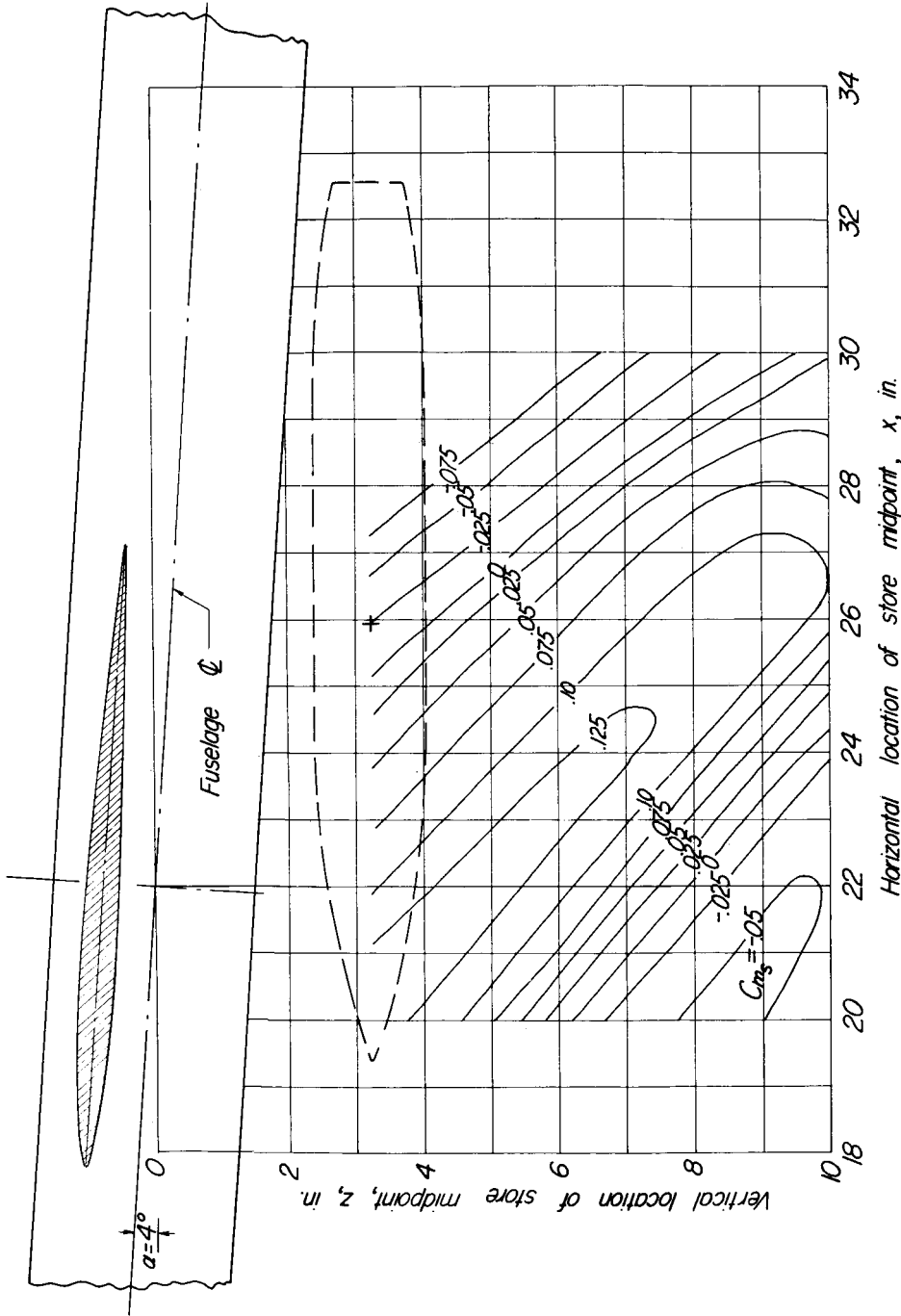
(d)  $\alpha_{WF} = 4^\circ$ ;  $\alpha_S = -4^\circ$ .

Figure 11.- Continued.



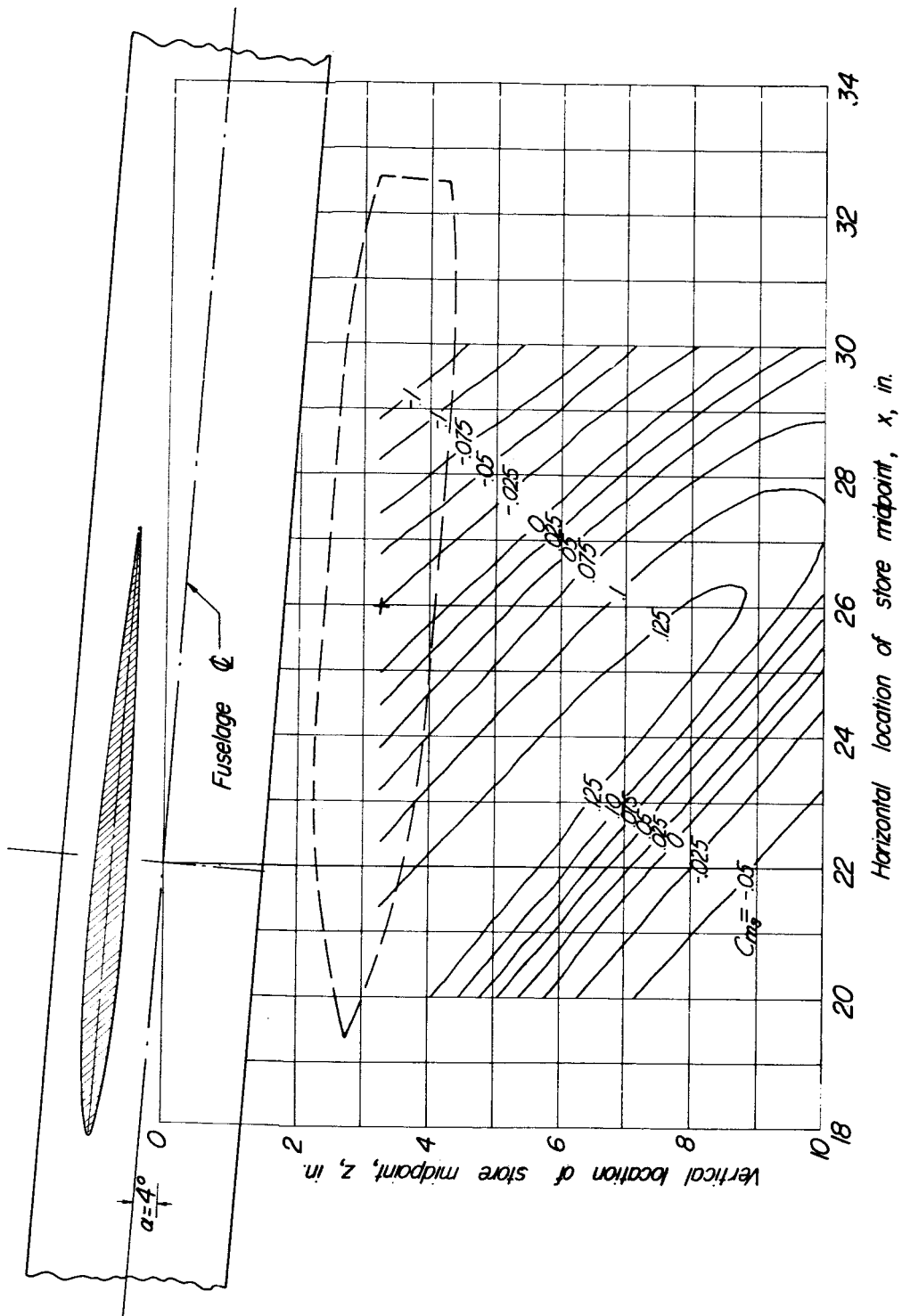
(e)  $\alpha_{wf} = 4^\circ$ ;  $\alpha_s = -8^\circ$ .

Figure 11.- Concluded.



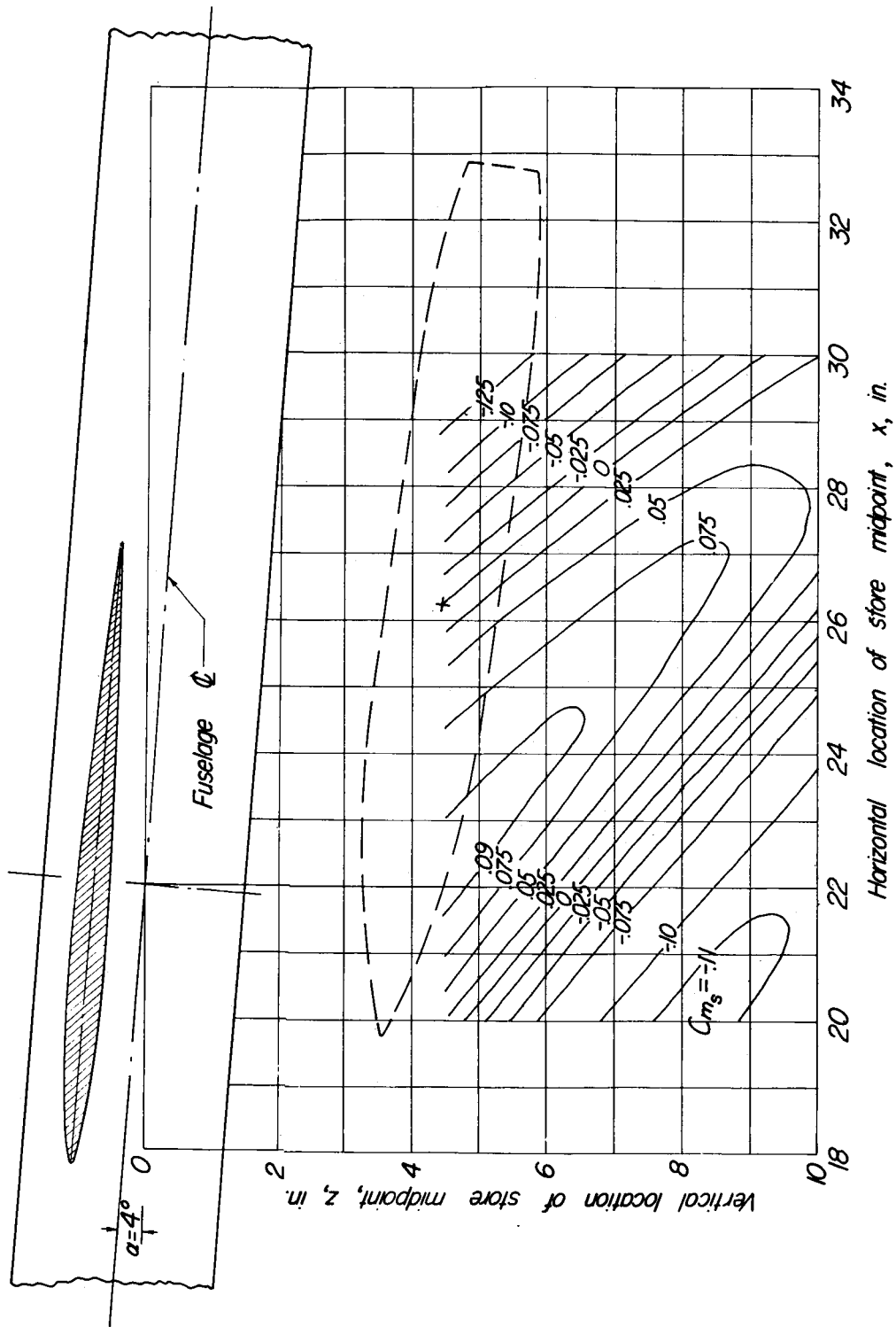
(a)  $\alpha_{wf} = 4^\circ$ ;  $\alpha_s = 0^\circ$ .

Figure 12.- Vertical contour plot of store pitching-moment coefficient in presence of wing-fuselage combination. (Wing section shown at fuselage surface.)



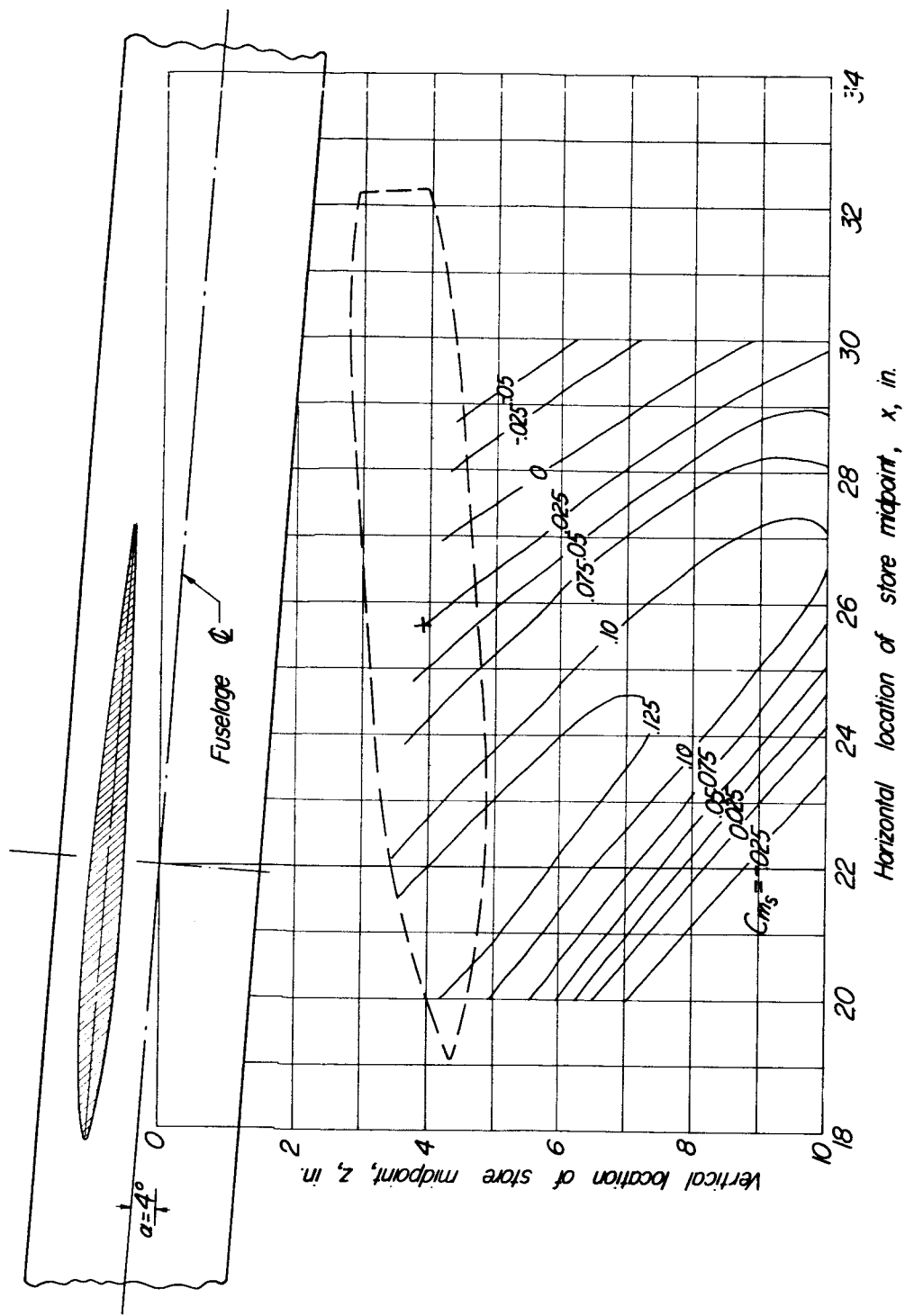
(b)  $\alpha_{wf} = 4^\circ$ ;  $\alpha_s = 4^\circ$ .

Figure 12.- Continued.



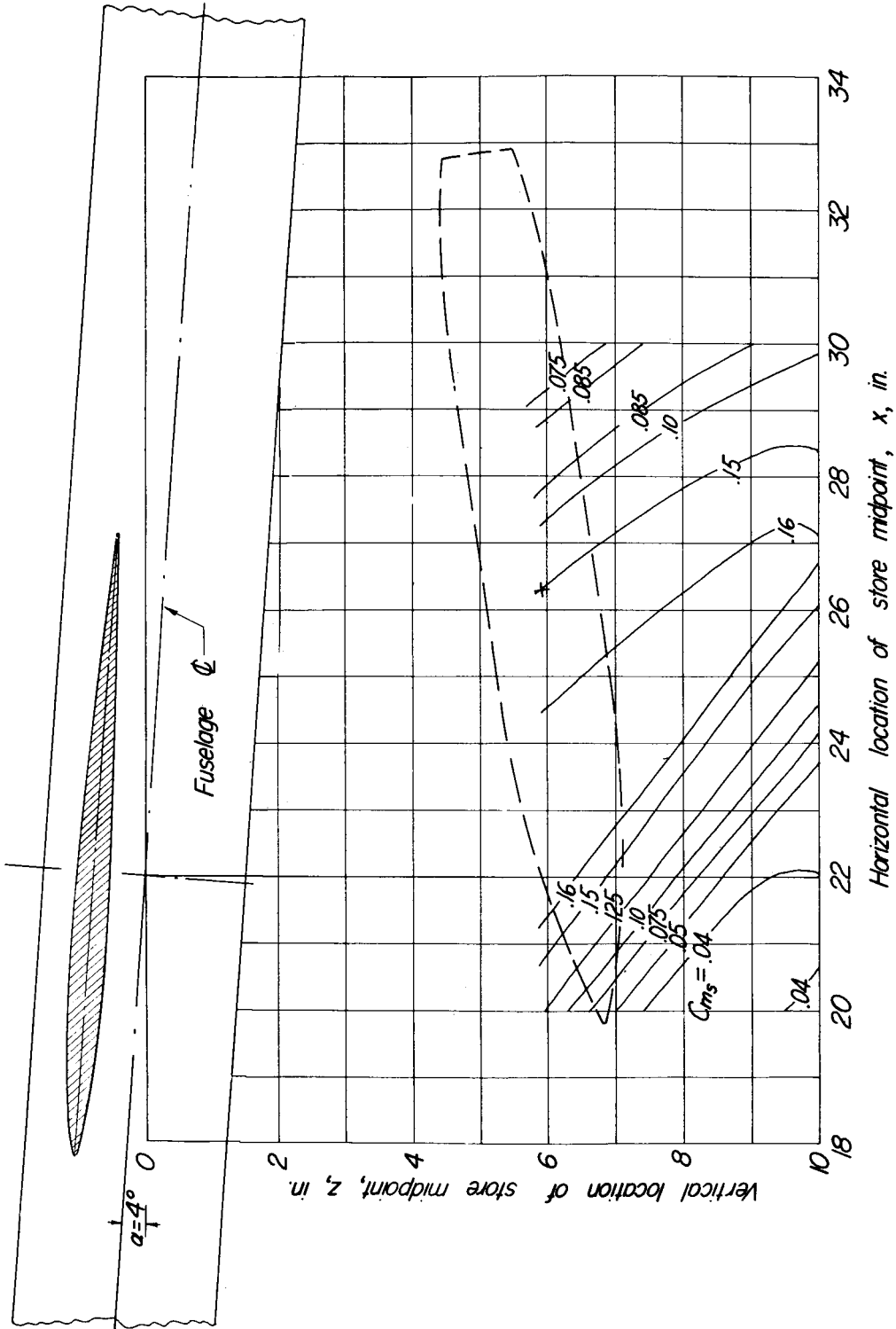
(c)  $\alpha_{WF} = 4^\circ$ ;  $\alpha_S = 8^\circ$ .

Figure 12.- Continued.



(d)  $\alpha_{WF} = 4^\circ$ ;  $\alpha_S = -4^\circ$ .

Figure 12.- Continued.



(e)  $\alpha_{wrf} = 4^\circ$ ;  $\alpha_s = -8^\circ$ .

Figure 12.- Concluded.